

# SPIN ANGULAR MOMENTUM OF 3D POLARIZATION STATES

José J. GIL

*University of Zaragoza, Pedro Cerbuna 12, 50009 Zaragoza, Spain*

Keywords: polarization, 3D polarization states, spin angular momentum of light

Although for a given point in the space, and for time intervals smaller than the coherence time of a given electromagnetic wave, the electric field describes a well-defined *polarization ellipse*, in general it is not stable for typical measurement times (usually much higher than the coherence time). Such lack stability of the polarization ellipse can affect to its size (intensity fluctuations), to its shape (depolarization) and to the plane containing it (3D states). Under the second-order approach, any polarization state (3D) or (2D) can be represented by means of its corresponding polarization matrix  $\mathbf{R}$ , whose elements are given by second order moments of the field variables [1]. Even though  $\mathbf{R}$  depends, in general, on nine independent parameters, it can be represented with respect to the so-called intrinsic reference frame  $X_oY_oZ_o$  [2] in such a manner that the *intrinsic polarization matrix*  $\mathbf{R}_o$  [2,3] depends on only six parameters, namely the intensity  $I$ , the degree of linear polarization  $P_l$ , the degree of directionality  $P_d$ , and the three components  $(n_{o1}, n_{o2}, n_{o3})$  of the *spin angular momentum*  $\mathbf{n}_o$  of the wave along the respective axes  $X_oY_oZ_o$  [3].

A meaningful classification of the polarization states can be performed on the basis of the characteristic (or trivial) decomposition of  $\mathbf{R}_o$  [4]

$$\mathbf{R}_o = P_1 I \hat{\mathbf{R}}_p + (P_2 - P_1) I \hat{\mathbf{R}}_m + (1 - P_2) I \hat{\mathbf{R}}_{u-3D}$$

$$\mathbf{R}_o \equiv I \hat{\mathbf{R}}_o = I \mathbf{U}_o \text{diag}(\hat{\lambda}_1, \hat{\lambda}_2, \hat{\lambda}_3) \mathbf{U}_o^\dagger \quad (1)$$

$$\hat{\mathbf{R}}_p \equiv \mathbf{U}_o \text{diag}(1, 0, 0) \mathbf{U}_o^\dagger \quad \hat{\mathbf{R}}_m \equiv \frac{1}{2} \mathbf{U}_o \text{diag}(1, 1, 0) \mathbf{U}_o^\dagger \quad \hat{\mathbf{R}}_{u-3D} \equiv \frac{1}{3} \mathbf{I}_3$$

where  $\hat{\lambda}_i$  are the eigenvalues of the normalized polarization matrix  $\hat{\mathbf{R}}_o \equiv \mathbf{R}_o/I$ ,  $\mathbf{U}_o$  is the unitary whose columns are the eigenvectors of  $\hat{\mathbf{R}}_o$ ,  $\mathbf{I}_3$  is the 3×3 identity matrix and  $(P_1, P_2)$  are the *indices of polarimetric purity* of  $\mathbf{R}_o$ , defined as [4,5,6]

$$P_1 = \hat{\lambda}_1 - \hat{\lambda}_2 \quad P_2 = \hat{\lambda}_1 + \hat{\lambda}_2 - 2\hat{\lambda}_3 \quad (2)$$

The above-mentioned classification requires the use of the following descriptors [2]

$$r \equiv \text{rank } \mathbf{R}_o = \text{rank } \mathbf{R} \quad t \equiv \text{rank}[\text{Re}(\mathbf{R}_o)] = \text{rank}[\text{Re}(\mathbf{R})] \quad m \equiv \text{rank}[\text{Re}(\mathbf{R}_m)] \quad (3)$$

and allows for an appropriate interpretation of the properties of  $\mathbf{n}_o$  for each case.

- [1]. J. J. Gil, R. Ossikovski, *Polarized light and the Mueller matrix approach*. CRC Press, 2016.
- [2]. J. J. Gil, Phys. Rev. A **90**(4), 043858-11 (2014).
- [3]. J. J. Gil, J. Opt. Soc. Am. A **33**(1), 40-43 (2016).
- [4]. J. J. Gil, Eur. Phys. J. Appl. Phys. **40**(1), 1-47 (2007).
- [5]. J. J. Gil, J. M. Correas, P. A. Melero, C. Ferreira, Monog. Sem. Mat. G. Galdeano **31**, 161–167 (2004).  
(available from [http://www.unizar.es/galdeano/actas\\_pau/PDFVIII/pp161-167.pdf](http://www.unizar.es/galdeano/actas_pau/PDFVIII/pp161-167.pdf)).
- [6]. I. San José, J. J. Gil, Opt. Commun. **284**(1), 38–47 (2011).

# **POSSIBILITIES FOR VORTEX STRUCTURES IN RANDOM LIGHT BEAMS**

Olga KOROTKOVA

*<sup>1</sup>Departement of Physics, University of Miami, Miami, Florida, USA*

Keywords: singular optics, random light beams, vortex structures

Modeling and laboratory generation of random sources that radiate light with arbitrary polar dependence of average intensity and polarization properties into the far zone is discussed. We show that the non-zero imaginary part of the source degree of coherence (in scalar case) and source degrees of correlations in polarization components (EM case) account for such far-field properties. As special cases vortices in average intensity and degree of polarization of any order are discussed. We also present a model for a scalar random source with a twist phase that radiates a beam with rotating average intensity.

## SPIN-ORBIT INTERACTIONS OF LIGHT IN ASYMMETRIC BEAMS

Nazar AL-WASSITI<sup>1</sup>, Evelina BIBIKOVA<sup>1,2</sup>, Nataliya KUNDIKOVA\*<sup>1,2</sup>

<sup>1</sup>South Ural State University, 76 Lenin Av., Chelyabinsk, Russia;

<sup>2</sup>Institute of Electrophysics of UD RAS, 106 Amundsen St., Yekaterinburg, Russia

Keywords: light beams, polarization, orbital angular momentum, spin-orbit interaction of light

Light beams can carry three types of angular momentum. The spin angular momentum is associated with polarization [1], the extrinsic orbital angular momentum is determined by the propagation path of the light beam [2], and the intrinsic orbital angular momentum is determined by the structure of the light field of the beam [3,4]. The effect of one of the angular momenta on another angular momentum leads to the spin-orbit interactions of light [5]. These effects can be observed under reflection and refraction of light beams, in focused light beams, under light propagation in anisotropic inhomogeneous medium and in optical fibers.

The spin-orbit interactions of light occur due to the translational or cylindrical symmetry breaking [6,7]. The effect of the spin angular momentum on the extrinsic orbital angular momentum in asymmetric light beams is the result of the cylindrical symmetry breaking. This effect was observed as the shift of the  $z$ -component of the asymmetric beam waist under the circular polarization sign change [8]. The asymmetric beam was formed by the screening of the half of Gaussian beam [8].

Here we present the results of the beam waist shift under the circular polarization sign change of Gaussian beam and Bessel beam carrying orbital angular momentum. The beams propagated through the upper part of a lens. The experimental setup is shown in Fig.1.

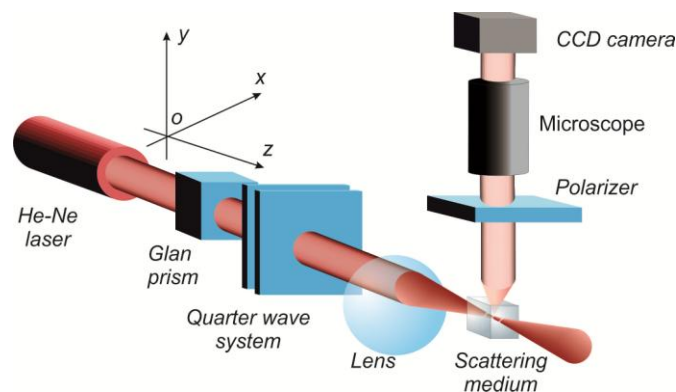


Fig. 1: experimental setup

We were successful to observe the waist shift of the  $z$ -component of Gaussian beam and Bessel beam under the circular polarization sign change.

- [1]. R. A. Beth, *Phys. Rev.*, **50**, 115-125 (1936)
- [2]. L. D. Landau, E. M. Lifshitz, E. M. Lifshitz, V. B. Berestetskii, L. P. Pitaevskii, V. B. Berestetskij, and L. P. Pitaevskij, *Course of Theoretical Physics. 4: Quantum Electrodynamics* (Pergamon Press, 1982)
- [3]. L. Allen, M.W. Beijersbergen, R.J.C. Spreeuw, J.P. Woerdman, *Phys. Rev. A*, **45**, 8185-8189 (1992)
- [4]. K. Bliokh, *Phys. Rev. Lett.*, **97**, 043901 (2006)
- [5]. S. Abdulkareem, N. Kundikova, *Opt. Express*, **24**, 19157-19166 (2016)
- [6]. N. Kundikova, *Proc. SPIE*, **3749**, 136-137 (1999)
- [7]. K. Y. Bliokh, F. J. Rodríguez-Fortuño, F. Nori, and A. V. Zayats, *Nat. Photonics* **9**, 796-808 (2015)
- [8]. B. Zel'dovich, N. D. Kundikova, and L. F. Rogacheva, *JETP Lett.* **59**, 766-769 (1994)

## **SATURATED NEGATIVE AND COMPLEMENTARY SPECKLE PATTERNS**

Marc GUILLON<sup>1</sup>, Jérôme GATEAU<sup>2</sup>, Marco PASCUCCI<sup>1</sup>, Hervé RIGNEAULT<sup>3</sup>,  
Gilles TESSIER<sup>2</sup>, Valentina EMILIANI<sup>1</sup>

<sup>1</sup>*Institute of Applied Physics RAS, Uljanov St.46, Nizhny Novgorod, Russia;*

<sup>1</sup>*Wavefront engineering group, Neurophotonics Laboratory, CNRS UMR 8250, University Paris Descartes, Sorbonne Paris Cité, Paris, France;*

<sup>2</sup>*Digital holography microscopy group, Neurophotonics Laboratory, CNRS UMR 8250, University Paris Descartes, Sorbonne Paris Cité, Paris, France;*

<sup>3</sup>*Aix-Marseille University, CNRS, Centrale Marseille, Institut Fresnel UMR 7249, Marseille, France*

Keywords: speckle patterns, super-resolution microscopy

Scalar wavefields passing through random media generate random speckle patterns. These patterns contain hot spots but also true zeros of intensity which draw lines in three-dimensional space [1]. For optical wavefields of high numerical apertures, the contribution of all three components of the field must be taken into account. In particular, the axial field cannot be neglected. In Stimulated Emission Depletion (STED) microscopy for instance [2], resolution is improved by stimulating fluorescence with a donut-shaped beam exhibiting an optical vortex at its dark center. This beam must be circularly polarized in order to cancel the axial component of the field at the center of the donut. Using the opposite “wrong” circular polarization yields a significant axial component resulting in deexciting fluorophores located at the donut center. Here, we image saturated negatives of high-NA speckle patterns thanks to super-resolution STED microscopy [3]. To do so, a uniformly fluorescent sample is photo-bleached by a speckle pattern prior to imaging. Zeros of intensity then appear as bright spots centered on optical vortices. Their topological charge is experimentally determined from negative patterns playing with circular polarization, thus allowing the observation of creation and annihilation processes along the propagation axis. In addition, the ability of vortices of speckle pattern to confine fluorescence to sub-diffraction dimensions is demonstrated, paving the way to novel super-resolution imaging techniques through turbid media [4]. A microscope scheme based on complementary speckle patterns [5], where intensity maxima and zeros are exchanged, is proposed.

[1] J. Nye and M. Berry, Proc. Roy. Soc. London A 336,165-190 (1974)

[2] S.W. Hell and J. Wichmann, Opt. Lett. 19, 780-782 (1994)

[3] M. Pascucci, G. Tessier, V. Emiliani, M. Guillon, Phys. Rev. Lett. 116, 093904 (2016)

[4] J. Bertolotti, E.G. van Putten, C. Blum, A. Lagendijk, W.L. Vos and A.P. Mosk, Nat. Methods 491, 232 (2012)

[5] J. Gateau, H. Rigneault, M. Guillon, arXiv:1607.06722 (2016)

## **GENERATING OAM FIELDS AND OTHER TYPES OF POLARIZATION DISTRIBUTIONS WITH LIQUID CRYSTAL ELEMENTS**

Gerben BOER

*Arcoptix, Rue de la Maladière 71, Neuchâtel, Switzerland;*

Keywords: polarization, optical angular momentum, liquid crystal elements

We will present different fabrication methods and devices based on liquid crystal (LC) technology that permits to obtain various types of circular symmetric polarization distributions. The optical axis of liquid crystal device can be structured either with a rubbing technic or with photo-alignment technics. This later alignment technic gives a whole range of possibilities for the design of structured birefringent elements. Additionally those LC elements can be made variable by adding transparent electrodes to the device and applying electrical fields.

We will present some devices realized by Arcoptix that use LC technology such as for example various spiral plated that permits to generate OAM fields, the well-known polarization converter (radial polarization) or a newly developed achromatic pi phase step plate.

## Holographic generation of highly focused vector fields with arbitrary polarization

Rosario MARTINEZ-HERRERO,<sup>1</sup> David MALUENDA,<sup>1</sup> Ignasi JUVELLS,<sup>2</sup>  
Artur CARNICER\*,<sup>2</sup>

<sup>1</sup>*Departamento de Óptica, Facultad de Ciencias Físicas, Universidad Complutense de Madrid, Ciudad Universitaria s/n, 28040 Madrid, Spain;*

<sup>2</sup>*Universitat de Barcelona, Facultat de Física, Departament de Física Aplicada, Martí i Franquès 1, 08028 Barcelona, Spain*

Keywords: Highly focused fields; Polarization; Computer holography.

Three dimensional electromagnetic field distributions generated at the focal region of a high numerical aperture (NA) focused system has been extensively investigated in the last years [1–6]. Non-paraxial fields have demonstrated very useful in many fields for instance in high-resolution microscopy, particle trapping, high-density recording, tomography, electron acceleration, nonlinear optics, and optical tweezers. In this contribution we present our recent advances in designing highly focused beams with arbitrary amplitude distribution, polarization and topological charge. Fields are experimentally generated using a Mach-Zehnder-based optical setup [7]. The illuminating beam is split in two fields with orthogonal polarizations using a polarizing beam splitter. Every component is independently manipulated by means of spatial light modulator displaying computer generated holograms [8]. After recombination, the resulting paraxial beam displays the expected properties at a given plane. This field can be focused using a high numerical aperture microscope objective [9,10] and the polarization state of the beam can be analyzed by measuring the Stokes parameters. This approach has been tested using either polarized or partially polarized illumination [11]. Applications to optical encryption and security has also been considered [12,13].

- [1]. H. Wang, L. Shi, B. Lukyanchuk, C. Sheppard, and C. T. Chong, *Nat. Photon.* **2**, 501–505 (2008)
- [2]. A. Y. Bekshaev, *Cent. Eur. J. Phys.* **8**, 947–960 (2010)
- [3]. L. Shao, P. Kner, E. H. Rego and M. G. L. Gustafsson, *Nat. Methods* **8**, 1044–1046 (2011)
- [4]. F. Kenny, D. Lara, O. Rodríguez-Herrera, and C. Dainty, *Opt. Express* **20**, 14015–14029 (2012).
- [5]. A. Ambrosio, L. Marrucci, F. Borbone, A. Roviello and P. Maddalena, *Nat. Commun.* **3**, 989 (2012).
- [6]. X. Li, T. Lan, C. Tien and M. Gu, *Nat. Commun.* **3**, 998 (2012).
- [7]. D. Maluenda, I. Juvells, R. Martínez-Herrero, and A. Carnicer, *Opt. Express* **21**, 5432–5439 (2013).
- [8]. V. Arrizón, *Opt. Lett.* **28**, 1359–1361 (2003).
- [9]. R. Martínez-Herrero, I. Juvells, and A. Carnicer, *Opt. Lett.* **38**, 2065–2067 (2013).
- [10]. D. Maluenda, R. Martínez-Herrero, I. Juvells, and A. Carnicer, *Opt. Express* **22**, 6859–6867 (2014).
- [11]. R. Martínez-Herrero, D. Maluenda, I. Juvells, and A. Carnicer, *Opt. Express* **22**, 32419–32428 (2014).
- [12]. D. Maluenda, A. Carnicer, R. Martínez-Herrero, I. Juvells, and B. Javidi, *Opt. Express* **23**, 655–666 (2015).
- [13]. A. Carnicer, I. Juvells, B. Javidi, and R. Martínez-Herrero, *Opt. Express* **24**, 6793–6801 (2016)

## SPATIAL EVOLUTION OF DIFFERENTIAL MUELLER MATRIX IN TURBID MEDIA: A STOCHASTIC APPROACH

Vincent DEVLAMINCK, Jean-Michel CHARBOIS

*Université de Lille, CRIStAL, UMR 9189, 59650 Villeneuve d'Ascq, France*

Keywords: polarization, differential Mueller matrix, turbid medium

We show in this paper the existence of different regimes in spatial evolution of depolarization in turbid media characterized by a diagonal Mueller matrix (pure depolarizer). Experimental results previously published, already established the existence of a first regime where the depolarization follows a parabolic law with the thickness of stationary medium traveled by light [1-2]. New experiments firstly confirm the existence of a second regime which we have previously demonstrated [3-4] where the depolarization follows a linear law on a large scale. They also confirm the existence of much more complex evolution laws even under small-scale approximation. A stochastic approach is proposed to model the phenomenon. It perfectly describes all these different experimental results and allows to analyze the behavior of the polarization in the case of solid or liquid scattering media. Entries of the depolarizing differential Mueller matrix (*DDMM*) are associated to fluctuation of birefringence and dichroism properties. These fluctuations are described by a stochastic Orstein-Uhlenbeck process:

$$X(z) = e^{-a(z-z_0)} X_0 + \int_{z_0}^z \sigma e^{a(u-z)} dB(u)$$

where  $B$  stands for a Brownian process,  $a$  is a parameter specifying how strongly the system reacts to perturbations and  $\sigma$  is related to the amplitude of the perturbation. Under small-scale approximation the diagonal entries  $\alpha_i$  of the *DDMM* are given by ( $Var(X_0)$  stands for the variance of  $X_0$ ):

$$\alpha_i = Var(X_0)z^2 + \left( \frac{\sigma^2}{3} - a \cdot Var(X_0) \right) z^3 \quad \text{with } 0 \leq Var(X_0) \leq \frac{\sigma^2}{2a}$$

Thus leading to changes that can continuously go from a parabolic behavior towards a cubic behavior depending on the value of  $Var(X_0)$ . This latter parameter can be related to the measurement setup and particularly to the numerical aperture used at the sample output for collecting light.

- [1]. R. Ossikovski, O. Arteaga, *Opt. Letters*. **39**, 4470-4473 (2014)
- [2]. N. Agarwal, J. Yoon, E. Garcia-Caurel, T. Novikova, J. Vanel, A. Pierangelo, A. Bykov, A. Popov, I. Meglinski, and R. Ossikovski *Opt. Lett.* **40**, 5634-5637 (2015).
- [3]. V. Devlaminck, *J. Opt. Soc. Am.* **30**, 2196-2204 (2013)
- [4]. V. Devlaminck, *J. Opt. Soc. Am. A* **32**, 1736-1743 (2015).

## Transport and depolarization of light in multiple scattering media

Rémi CARMINATI,\*<sup>1</sup> Romain PIERRAT,<sup>1</sup> Kevin VYNCK <sup>2</sup>

<sup>1</sup>*Institut Langevin, ESPCI Paris, PSL Research University, CNRS, 1 rue Jussieu, 75005 Paris, France;*

<sup>2</sup>*LP2N, CNRS, Institut d'Optique Graduate School, University of Bordeaux, 33400 Talence, France*

Keywords: optics, multiple scattering, polarization, depolarization length

The analysis of coherence and polarization of multiply scattered light has become an important issue, stimulated by the development of advanced imaging techniques, and by fundamental questions, as the definition of spatial coherence and polarization degrees in three-dimensional speckles [1,2]. In this work we analyse the diffusion of polarized light in multiple scattering media, and the length scales involved in the depolarization process. An interesting outcome of the formalism is the introduction of diffusion “polarization eigenmodes” [3], that are characterized by specific transport mean free paths, and specific attenuation lengths. The transport mean free path of each eigenmode depends nontrivially on the anisotropy factor  $g$ , thus establishing a connection between the depolarization length scales and the microstructure of the medium.

[1]. A. Dogariu and R. Carminati, Phys. Rep. 559, 1 (2015).

[2]. Ph. Réfrégier, V. Wasik, K. Vynck and R. Carminati, Opt. Lett. 39, 2362 (2014)

[3]. K. Vynck, R. Pierrat and R. Carminati, Phys. Rev. A 89, 013842 (2014)

[4]. K. Vynck, R. Pierrat and R. Carminati, Phys. Rev. A 94, 033851 (2016)

## Single biaxial crystal based snapshot polarimeters

Angel LIZANA\*<sup>1</sup>, Irene ESTÉVEZ<sup>1</sup>, Alex TURPIN<sup>1</sup>, Alba PEINADO<sup>1</sup>, Victor SOPO<sup>1</sup>,  
Claudio RAMIREZ<sup>1</sup>, Juan CAMPOS<sup>1</sup>

<sup>1</sup>*Departament de Física, Universitat Autònoma de Barcelona, 08193, Bellaterra, Spain*

Keywords: Stokes polarimeter, snapshot, biaxial crystal, conical refraction

Polarimetric information is of interest in a widespread range of applications [1], as in astronomy, remote sensing, materials characterization, etc. For real-time applications, one of the key parameters is the velocity, so snapshot polarimeters (SP) are required. In this last case, most of the SP we found in literature are based in amplitude-division or wavefront-division schemes. Recently, some authors have shown the interest of one particular amplitude division polarimeter which is based on the conical refraction (CR) phenomenon occurring in biaxial crystals (BC). In particular, when a focused beam propagates along one of the optical axis of a biaxial crystal the CR is produced, this leading to a ring-like intensity distribution at the focal plane. More importantly for our interests, the polarization distribution of the obtained light ring is directly linked with the polarization of the input beam.

At the moment, most of the optical architectures provided for BC polarimeters include two optical arms with a BC each. This necessity arises from the fact that polarimetric content provided by a BC is restricted to linear polarization. Thus, the extra arm properly combines a retarder with the second BC, this allowing complete polarimetry. In addition, to achieve complete polarimetry, two CCD cameras are also required, with a proper synchronization between them.

In this work we present two different optical architectures for the implementation of BC polarimeters, which only require of one BC [2,3]. The presented schemes not only reduce costs when compared with other proposal, but also are based on faceable optical arrangements. In particular, one of the configurations leads to an incomplete polarimeter (linear detection), while the other configuration leads to a complete polarimeter. Both polarimeters are implemented and experimentally tested by measuring different known input polarizations. Their performances are discussed in terms of accuracy and repeatability.

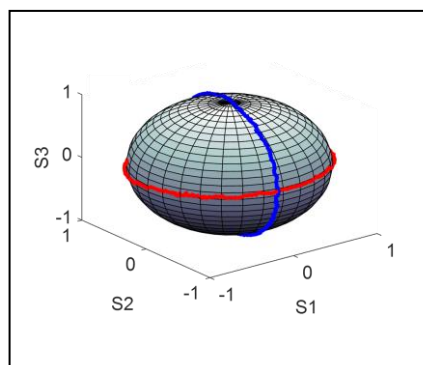


Fig. 1: BC polarimeter polarization analyzers

- [1]. F. Snik, J. Craven-Jones, M. Escuti, S. Fineschi, D. Harrington, A. De Martino, D. Mawet, J. Riedi, J.S. Tyo, Proc. SPIE 9099, 90990B (2014)
- [2]. A. Lizana, I. Estévez, A. Turpin, C. Ramirez A. Peinado, J. Campos, Applied Optics 54(29), 8758-8765 (2015)
- [3]. I. Estévez, V. Sopo, A. Lizana, A. Turpin, J. Campos, Optics Letters 41(19), 4566-4569 (2016)

## Polarimetric imaging in chiral media

Oriol ARTEAGA<sup>1</sup>

<sup>1</sup> *Departament de Física Aplicada, FEMAN group, IN2UB, Universitat de Barcelona, C/ Martí i Franqués, 1 Barcelona 08030, Spain.*

Keywords: chirality, imaging, Mueller matrix polarimetry, spin angular momentum

This work reviews our recent progresses imaging of chiral media with Mueller matrix polarimetry. A comprehensive presentation of our method will be provided, detailing the instrumentation used for high resolution polarimetric imaging, a few remarks about data analysis and basic concepts about light propagation in chiral media. Despite chiral media is especially sensitive to the spin angular momentum, we will discuss how optical characterization methods based only in the use of circularly polarized light can often render inconclusive or erroneous results for chiral assessment. Mueller matrix imaging is an ideal method to unveil the complexity of inhomogeneous anisotropic media.

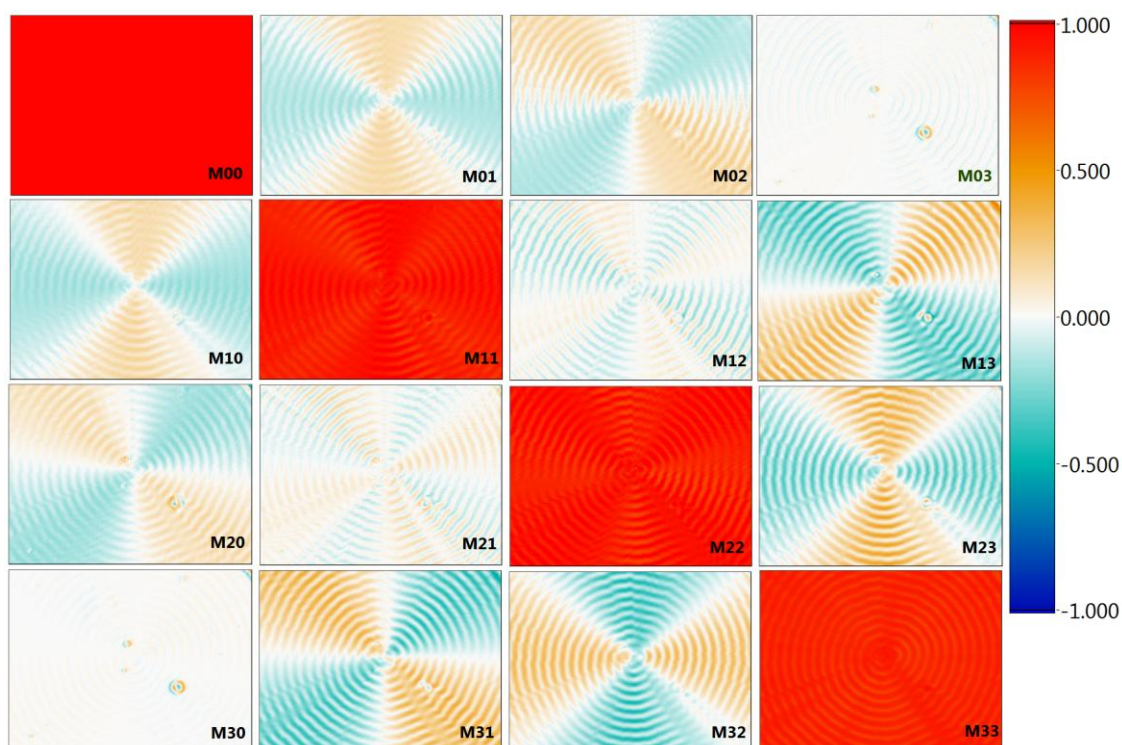


Fig. 1: Mueller matrix imaging of a mannitol spherulite made of twisted lamella, from Ref. [1]

[1]. X. Cui, S. Nichols, O. Arteaga, J. Freudenthal, F. Paula, A. Shtukenberg and B. Karh. *J. Am. Chem. Soc.* 138, 12211-12218 (2016).

## Comparison of the detection performance of static and adaptive polarization imagers

François GOUDAIL

*Laboratoire Charles Fabry, UMR 8501, Institut d'Optique Graduate School, CNRS, Univ Paris Sud  
11, 2 rue Augustin Fresnel, 91127 Palaiseau, France*

Keywords: optics, polarization, optical orbital momentum

A Stokes imager is a device that measures the polarization state of the light backscattered by each point of a scene, forming an image of its Stokes vector. The Stokes parameters are estimated from four intensity images formed by analyzing the light with four different polarization analysis devices. The optimal choice of these four polarization states in order to minimize the estimation variance of Stokes parameters has been long investigated [1-5]. It has been shown that they have to form a regular tetrahedron in the Poincaré sphere.

More recently, attention has been drawn on the fact that if the purpose is not to estimate Stokes vector, but to perform target detection from polarimetric measurements, the appropriate optimization criterion is the polarimetric contrast between an object of interest and the background [6]. In this case, the optimal strategy consists in acquiring a single image with an analysis state that is optimized with respect to the polarimetric properties of the two regions to discriminate [7]. However, to implement this optimal strategy, polarimetric imagers have to be able to adapt to the scene, and thus to generate any polarization state on the Poincaré sphere. Such adaptive polarimetric imaging devices have been developed [8]. They make it possible to maximize target detection performance at the price of increased complexity compared to static Stokes imagers implementing four predefined analysis states. In order to make a well-informed choice between a static imager and an adaptive one for a given application, one needs to be able to evaluate if the performance reached by the former is sufficient.

It is the purpose of the presented research work to investigate this issue. By using a minimax approach, we determine the set of analysis states of a static Stokes imager that maximizes target detection performance in the worst case, that is, the less favorable target-background configuration. We find it to be the same as the configuration that minimizes Stokes vector estimation error: the analysis states have to form a regular tetrahedron on the Poincaré sphere. In this configuration, the averaged value of the contrast on the four channels only depends on a single parameter which synthetically represents the "strength" of the polarimetric difference between the target and the background. We compare the contrast provided by the fully adaptive imager with the total contrast on the 4 channels of the static imager, and with the contrast of the best channel of the static imager. In particular, it is shown that the contrast of the best channel is, in the worst case, equal to one third of that provided by the fully adaptive imager. Considering that fully adaptive imagers are more difficult to build and calibrate, well-designed static imagers constitute an attractive alternative in applications where limited loss of discrimination ability can be tolerated.

- [1] R.M.A. Azzam, I.M. Elminyaw, A.M. El-Saba, *J. Opt. Soc. Am. A*, **5**, 681-689 (1988).
- [2] A. Ambirajan, D. C. Look, *Opt. Eng.*, **34**, 1656-1658 (1995).
- [3] D. S. Sabatke et al., *Opt. Lett.*, **25**, 802-804 (2000).
- [4] J. S. Tyo, *Appl. Opt.*, **41**, 619-630 (2002).
- [5] F. Goudail, *Opt. Lett.*, **34**, 647-649 (2009).
- [6] F. Goudail, A. Bénéière, *Opt. Lett.* **34**, 1471-1473 (2009).
- [7] F. Goudail, *Opt. Lett.*, **35**, 2600-2602 (2010).
- [8] G. Anna, H. Sauer, F. Goudail, and D. Dolfi, *Applied Optics*, **51**, 5302-5309 (2012).

## FROM MOLECULES TO META-MOLECULES FOR NONLINEAR OPTICS

Clément LAFARGUE<sup>1</sup>, Radek KOLKOWSKI<sup>1</sup>, Joseph ZYSS<sup>1</sup>

*Laboratoire de Photonique Quantique et Moléculaire (CNRS 8537) et Institut d'Alembert  
Ecole Normale Supérieure de Paris-Saclay, Cachan, France*

Keywords: plasmonics, nanotechnology, nonlinear optics, nano-cavities second-harmonic generation, chirality, meta-molecules

Molecular engineering for NLO has experienced a first revival from the early nineties to this day, when its scope was enlarged from a more restricted earlier blueprint of donor-acceptor dipolar entities, to encompass the broader pool of multipolar molecules, following tensor symmetry guidelines. In the wake of the development of nanotechnologies and nano-sciences, the field of nano-plasmonics appeared, more recently as a further enlarged playground for molecular engineering, with the early proposition of octupolar associations of nanoparticles [1] showing the way towards up-scaled and enhanced nonlinear optical entities, in both 2-D and 3-D arrangements. Over recent years, the concept of « meta-molecules » has emerged, by way of associating « meta-atomic » building blocks in the form of either metallic nano-cavities [2] or nanoparticles [3] down to a typical 200nm scale and less. This second revival has been guided, like the previous one, by combining fundamental group symmetry and tensor arguments, applied now in the different physical frame of plasmonics, entailing the additional challenge of non-local interactions. The interplay between localized plasmons and propagative ones has led to interesting associations from nano-particles and nano-cavities, onto meta-molecular associations of these, all the way to meta-arrays [4]. The implementation of chirality is further leading to interesting possibilities towards high-density data encryption [5]. Polarization resolved nonlinear confocal microscopy [6] stands-out in the toolbox that we have conceived and developed over the last decade towards nonlinear optical characterization down to single nano-scale nonlinear entities.

I will survey the different steps of this ongoing story, from theoretical, experimental and technological viewpoints, covering basics all the way to current advances in our laboratory.

- [1] M. I. Stockman, K. Li, S. Brasselet, J. Zyss, Octupolar metal nanoparticles as optically driven, coherently controlled nanorotors. *Chem. Phys. Lett.* 433, 130–135 (2006)
- [2] A. Salomon, Y. Prior, M. Fedoruk, J. Feldmann, R. Kolkowski, J. Zyss, Plasmonic coupling between metallic nanocavities, *J. Opt.* 16, 114012 (2014)
- [3] R.Hou, V.Shynkar, C.Lafargue, J.Zyss, Lagugné Labarthe JPPC (2016)
- [4] R.Kolkowski, J.Szesko, B.Dwir, E.Kapon, J.Zyss, Non-centrosymmetric plasmonic crystals for second-harmonic generation with controlled anisotropy enhancement, *Laser Photonics Review*, (2016)
- [5] R. Kolkowski, L. Petti, M. Rippa, C. Lafargue, J. Zyss, Octupolar plasmonic meta-molecules for nonlinear chiral watermarking at subwavelength scale, *ACS Photonics* 2, 899–906 (2015)
- [6] S. Brasselet, V. Le Floch, F. Treussart, J. F. Roch, A. Ibanez, J. Zyss, In-situ diagnostics of the crystalline nature of single organic nanocrystals by nonlinear microscopy, *Phys. Rev. Lett.* 92(20), 207401 (2004)

# Dynamics of DNA G-quadruplex structures by time-resolved circular dichroism

Marco Schmid, Pascale Changenet-Barret, and François Hache

*Laboratoire d'Optique et Biosciences  
Ecole Polytechnique, CNRS, INSERM  
91128 Palaiseau cedex, France*

G-quadruplexes are DNA structures composed of stacked guanine quartets which are of growing interest due to their prevalence in many important regions, such as telomeres and regulatory regions of many oncogene promoters [1]. Manipulation and stabilization of these DNA structures by specific ligands establish a new and promising field of cancer therapeutics. In this paper, we investigate the folding/unfolding equilibrium of the quadruplex Tel21 (TTA(GGGTTA)<sub>3</sub>) by time-resolved absorption and circular dichroism measurements coupled with a T-jump experiment [2]. Circular dichroism spectroscopy is performed thanks to an original technique where a unique pulse serves as probe for the absorption of right and left-polarized light, yielding self-referenced signals.

Directly after heating by a nanosecond IR laser pulse, an increase in absorption and circular dichroism takes place which is assigned to base unstacking. This is followed by a decrease reflecting the unfolding dynamics. Investigations on dynamics for larger time scales are expected to reveal more information and confirm further our results.

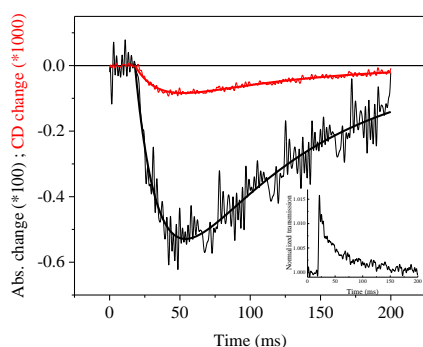


Figure 1 : Change in absorption and circular dichroism at 293 nm following a 5°C temperature jump.

[1] J. Huppert, *Phil. Trans. R. Soc. A* **365**, 2969 (2007).

[2] L. Mendonça, A. Steinbacher, R. Bouganne, F. Hache, *J. Phys. Chem. B* **118**, 5350 (2014)

## **MEASUREMENT OF SMALL LIGHT ABSORPTION IN MICROPARTICLES BY MEANS OF OPTICALLY INDUCED ROTATION**

Oleg V. ANGELSKY<sup>1</sup>, Yuriy USHENKO<sup>1</sup>, Alexandre. Y. BEKSHAEV<sup>2</sup>, Petr P. MAKSIMYAK<sup>1</sup>, Alexandre. P. MAKSIMYAK<sup>1</sup>, and Steen G. HANSON<sup>3</sup>

<sup>1</sup>*Correlation Optics Department, Chernivtsi National University, Chernivtsi 58012, Ukraine;*

<sup>2</sup>*Research Institute of Physics, Odessa I.I. Mechnikov National University, Odessa, Ukraine;*

<sup>3</sup>*DTU Fotonik, Department of Photonics Engineering, DK-4000 Roskilde, Denmark*

Keywords: optics, light absorption, optical orbital momentum

The absorption parameters of micro-particles have been associated with the induced spin exerted upon the particle, when embedded in a circularly polarized coherent field. The induced rotational speed is theoretically analyzed, showing the influence of the beam parameters, the parameters of the particle and the tribological parameters of the surrounding fluid. The theoretical findings have been adequately confirmed in experiments.

## **Circular polarization memory in multiple scattering media and associated similarity relations**

Callum MACDONALD\*,<sup>1,2</sup>

<sup>1</sup>*Aix Marseille Université, CNRS, Centrale Marseille, Institut Fresnel UMR 7249, 13013 Marseille, France;*

<sup>2</sup>*Department of Physics, University of Otago, Dunedin 9016, New Zealand*

Keywords: circular polarization memory, chirality, depolarization, similarity relations

Circular polarization memory has been previously observed in various scattering media, although characterizing this behaviour in complex media has proved challenging. This is a phenomena which fundamentally is enabled by the chiral nature of photon polarization states that carry spin angular momentum. The finer details of how circular polarization memory arises in certain scattering media are discussed, as well as a set of parameters which are capable of characterizing this behaviour. These parameters can be calculated for media having any arbitrary distribution of spherical scattering particles, in both size, and refractive index.

Results of simulations and experimental investigations are shown which point towards a similarity relationship that describes the spatially resolved backscattered Degree of Circular Polarization (DOCP) from optically dense media. This similarity relationship is analogous to the well known case in scalar radiative transport, where various media that are degenerate in terms of their absorption coefficients, and reduced scattering coefficients, share similar radiances for locations sufficiently distant from light sources. The similarity relationships shown here for the measurable DOCP, simply require additional parameters to be matched. This is further tested by exploring circular polarization memory in polydisperse media.

## ROTATING TWO-LOBE LIGHT FIELDS

Eugeny ABRAMOCHKIN<sup>1</sup>, Svetlana KOTOVA<sup>\*,1,2</sup>, Nikolay LOSEVSKY<sup>1</sup>,  
Darya PROKOPOVA<sup>1,2</sup>, Evgenia RAZUEVA<sup>1</sup>

<sup>1</sup>Lebedev Physical Institute, 221, Novo-Sadovaya Str., Samara, 443011, Russia;

<sup>2</sup>Samara National Research University 34, Moskovskoye shosse, Samara, 443086, Russia

Keywords: spiral light beams, rotation parameter, longitudinal super-resolution

Rotating two-lobe light fields, i.e. fields with a rotating intensity distribution under propagation, are of great interest for obtaining longitudinal super-resolution in fluorescent optical microscopes [1]. In this study the light fields under consideration were generated via spiral beam optics methods [2]. Spiral beams are paraxial light fields with a transverse intensity distribution which rotates around the beam axis maintaining its shape (but not the scale) whilst propagating. They can have different types of intensity distribution. The spiral beam's rotation angle,  $\theta$ , in a plane located at distance  $z$  from the initial position, is defined by the expression:

$$\theta(z) = \theta_0 \arctan\left(\frac{2z}{kw^2}\right),$$

where  $k$  is the wave number,  $w$  – transverse beam size,  $\theta_0$ – beam rotation parameter defining the speed of the beam rotation during propagation. The full rotation angle in the Fresnel zone is equal to

$\theta = \theta_0 \frac{\pi}{2}$ . Within this work we considered the light fields with the rotation parameters  $\theta_0 = -1, -2, -3, -4, -5$ , formed by the method of functional representation [3].

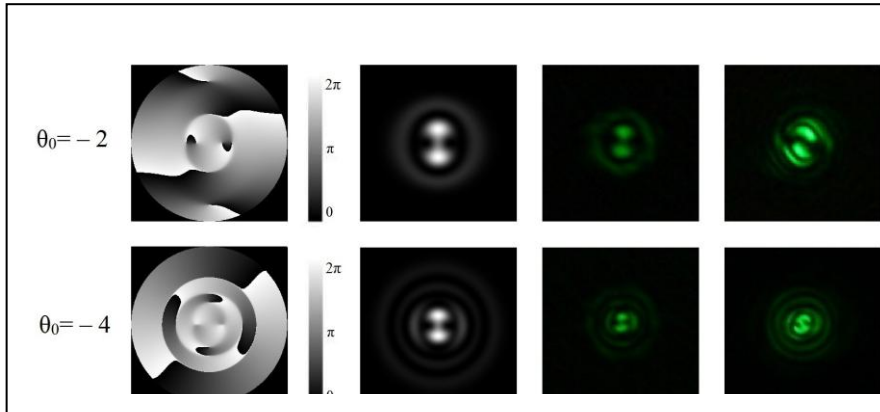


Fig. 1: (Left to right) Phase, theoretical and experimental intensity distributions of spiral beam; intensity distribution formed by appropriate phase mask

In our experiments the required spiral beams were obtained by using holographic technique. We have also studied the generation of light fields with the aid of phase masks with transmission profiles that replicate the phase distribution of the spiral beam. This is done to increase the energy efficiency of the light fields being formed. The power efficiency of the field generation and the dependencies for the intensity distribution rotation angle versus the distance from the focusing plane have been obtained. The results of simulation and experiments on the formation of the studied fields are in good agreement.

- [1]. M.D. Lew, M.A. Thompson, M. Badieirostami, W.E. Moerner, Proc. of SPIE, **7571**, 75710Z (2010)
- [2]. E.G. Abramochkin, V.G. Volostnikov, Uspekhi Fizicheskikh Nauk, **174**(12), 1273-1300 (2004)
- [3]. E.V Razueva, E.G. Abramochkin, EPJ Web of Conferences, **103**, 10011 (2015)

## EVALUATION OF POLARIZATION DIFFERENCE IMAGING AT A LONG WORKING DISTANCES

Yohann SILLAM<sup>1</sup>, Amir BERNAT<sup>1</sup>, David LEVITZ \*<sup>1</sup>

<sup>1</sup>*MobileODT Ltd., Gershon Shatz 41, Tel Aviv, Israel;*

Keywords: polarization difference imaging, skin imaging

Polarization difference imaging (PDI) is an optical imaging technique that can highlight pathologies in layered epithelial tissues. In this method, two polarized images are captured in which the polarizer and analyzer are parallel/orthogonal to one another, and the difference between them is calculated. The PDI image isolates the single scattered light reflected off the epithelium, allowing to better visualize abnormalities in this layer are otherwise hidden by diffuse light from deeper tissues. Earlier implementations<sup>1,2</sup> of PDI involved imaging the tissue in direct contact with a glass plate, in order to eliminate the specular reflection. However, PDI imaging from a distance has not been explored much. Such an analysis would help determine if the technology is suitable for medical imaging applications such as colposcopy, where the cervix is imaged from outside the patient's body.

In this paper, PDI imaging at a working distance of 30 cm is presented. Green (527 nm, Cree) LED is used to illuminate a polarimetric imaging system. Sequential parallel and orthogonal images are captured using a liquid crystal variable retarder (LCVR) as the polarizer. The camera and LCVR were controlled by a program written in MATLAB, which varied the LCVR voltage to alternate the polarization, while capturing successive frames on the camera. Images were captured in under 0.5 sec, to ensure a low rate of image misregistration. As in colposcopy imaging geometry, the glass plate would not added. This made the system more sensitive to specular reflections, but removed the risks of air bubble traps. Preliminary testing were performed on human skin and fruits.

The results show that despite specular reflection, non-contact PDI imaging even at a distance of 30 cm can eliminate light reflected from deep tissue, and highlight superficial layer features in the image. An example of unpolarized and PDI images of a nevus are shown in Fig. 1 alongside with corresponding pictures from earlier work done with glass plate in contact mode.<sup>1</sup> This suggests PDI imaging at a distance is suitable to identify superficial lesions in the epithelial layer, such as cervical dysplasia. Future work will adapt the PDI system described here onto a smaller form factor to enable mobile colposcopic PDI imaging.

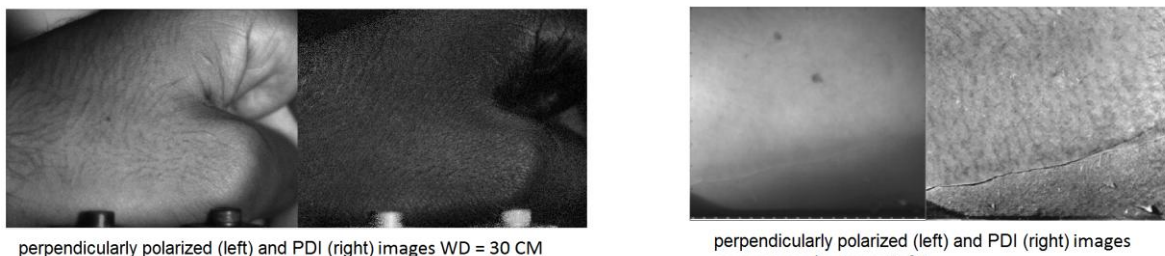


Fig. 1: Sample unpolarized and PDI images of a nevus, imaged at 30 cm (left) and in contact mode (right) from Jacques et al.<sup>1</sup>

- [1] Jacques S. L., & R.-R. Jessica, Imaging skin pathology with polarized light., *J Biomed Opt* **7(3)**, 329-340, (2002)
- [2] Samatham R., Lee K., Jacques S. Clinical study of imaging skin cancer margins using polarized light imaging. *Proc SPIE* 8207, 82070O-1-9 (2012).

## Reciprocity in vector radiative transport and the sensitivity of probing regions to various polarization imaging channels

Callum MACDONALD<sup>1,\*</sup>, Ugo TRICOLI<sup>1</sup>, Anabela DA SILVA<sup>1</sup>, Vadim MARKEL<sup>1</sup>

<sup>1</sup>Aix Marseille Université, CNRS, Centrale Marseille, Institut Fresnel UMR 7249, 130013 Marseille, France

Keywords: polarization, reciprocity, diffuse optical tomography, polarization gating

We have derived a reciprocity relation for the Vector Radiative Transport Equation (V-RTE), and have applied it in the calculation of the sensitivity kernel for polarized diffuse optical tomography measurements. This new formalism provides a unique ability to investigate the regions of a scattering medium that are most sensitive to various polarization imaging channels (having different combinations of filters for incident and detected light). In particular, we can explore the potential differences involved when probing with polarizations having angular momentum, i.e, circular or elliptical states.

The reciprocity relations we derive relate to the Green's functions of the V-RTE, and follow from the previously derived reciprocity relations for the single scattering phase matrix detailed by Hovenier [1]. These relations, along with additional symmetries inherent in certain experimental geometries, dramatically reduce the computational requirements for calculating the kernel of the sensitivity function for diffuse optical tomography with polarized light.

With the inclusion of polarization information in the tomographic problem, it is hoped that the ill-posedness of diffuse tomographic reconstruction is reduced. The derived formalism however also provides new insight into the sensitivity of different probing regions to polarization, which is of particular interest to the community involved with polarization gated imaging of highly scattering media (see example in Fig. 1).

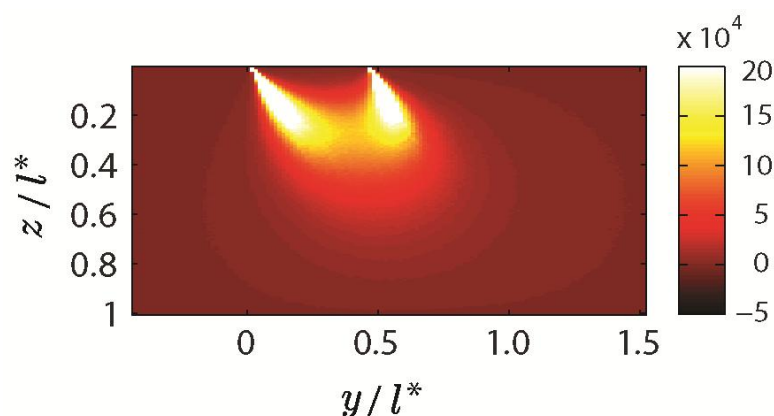


Fig. 1: Example of a kernel matrix element of the sensitivity function for polarized diffuse optical tomography (light source located on the left, detector on the right) . Results calculated via polarized Monte Carlo program.

[1]. J. W. Hovenier, J. Atmospheric Sci. **26**(3), 488-499 (1969)

## MEDIUM WITH ORTHOGONAL EIGENPOLARIZATIONS: DIFFERENTIAL APPROACH

Sergey SAVENKOV\*, Ivan KOLOMIETS, Yevgen OBEREMOK, Alexander KLIMOV

*Taras Shevchenko National University of Kyiv, Vladimirskaya str. 64, Kiev, Ukraine  
sns@univ.kiev.ua*

Keywords: polarization, Jones matrix, eigenpolarizations, birefringence, dichroism

Main goal of this paper is twofold: first, to obtain in scope of the differential Jones method the conditions under which the eigenpolarizations of arbitrary deterministic medium are orthogonal and, second, to conduct a comparative analysis of the obtained conditions and similar conditions obtained in scope of the generalized equivalence theorem decomposition [1,2].

The eigenpolarization orthogonality conditions in scope of the differential Jones method are follows

$$\begin{cases} \delta = -\varphi \ln(P) / \operatorname{arctanh}(R) \\ \alpha = \theta \end{cases}, \quad (1)$$

where  $\delta$  and  $\alpha$  - value and azimuth of linear birefringence;  $\varphi$  - value of circular birefringence;  $P$  and  $\theta$  - value and azimuth of linear dichroism;  $R$  - value of circular dichroism.

Thus, Eq.(1) show that the “differential” orthogonality of eigenpolarizations is possible in the case of linear birefringence and dichroism collinearity only. At the same time, in scope of the generalized equivalence theorem decomposition this requirement is not mandatory [2]. However, we show that in scope of the generalized equivalence theorem decomposition there is also a solution satisfying the requirement of linear birefringence and dichroism collinearity and including all four elementary types of anisotropy.

Fig. 1 shows one more interesting feature of “differential” solution Eq.(1). This is the dependences of eigenpolarizations ellipticity  $\varepsilon$  on the values of linear  $P$  and circular  $R$  dichroism. It can be seen that for “differential” solution there exists a “bandgap” for  $\varepsilon$  in the vicinity of singular value of linear dichroism.

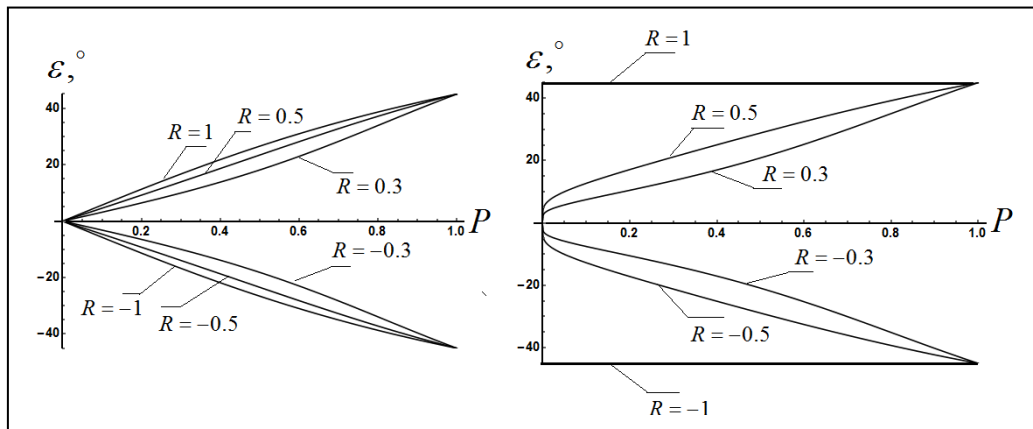


Fig. 1: Dependences of eigenpolarizations ellipticity  $\varepsilon$  on the values of linear  $P$  and circular  $R$  dichroism for multiplicative (left) and differential (right) Jones methods

[1]. S. Savenkov, V. Marienko, E. Oberemok, O. Sydoruk, Phys Rev E 74, 056607 (2006).

[2]. S. Savenkov, E. Oberemok, A. Kushchenko, I. Kolomiets, A. Klimov, Appl. Spect., 82(5), 801 (2015)

## DIFFERENTIAL PARTIAL JONES EQUIVALENCE THEOREMS

Sergey SAVENKOV\*, Ivan KOLOMIETS, Yevgen OBEREMOK, Alexander KLIMOV

Taras Shevchenko National University of Kyiv, Vladimirskaya str. 64, Kiev, Ukraine  
sns@univ.kiev.ua

Keywords: Jones matrix, generalized equivalence theorem, eigenvalues

We address the important problem noted firstly in [1], i.e., the performing a comparative analysis of the anisotropic parameters derived via the differential matrix decomposition and the multiplicative decomposition (specifically, the generalized equivalence theorem decomposition [2]), and establishing the interrelations between them. We have therefore obtained the explicit forms of direct and inverse relations between anisotropic parameters (i.e., linear and circular birefringence and dichroism) derived from the generalized equivalence theorem decomposition and the differential matrix decomposition.

Fig.1 illustrates obtained results on the example of the first and second Jones equivalence theorems [3].

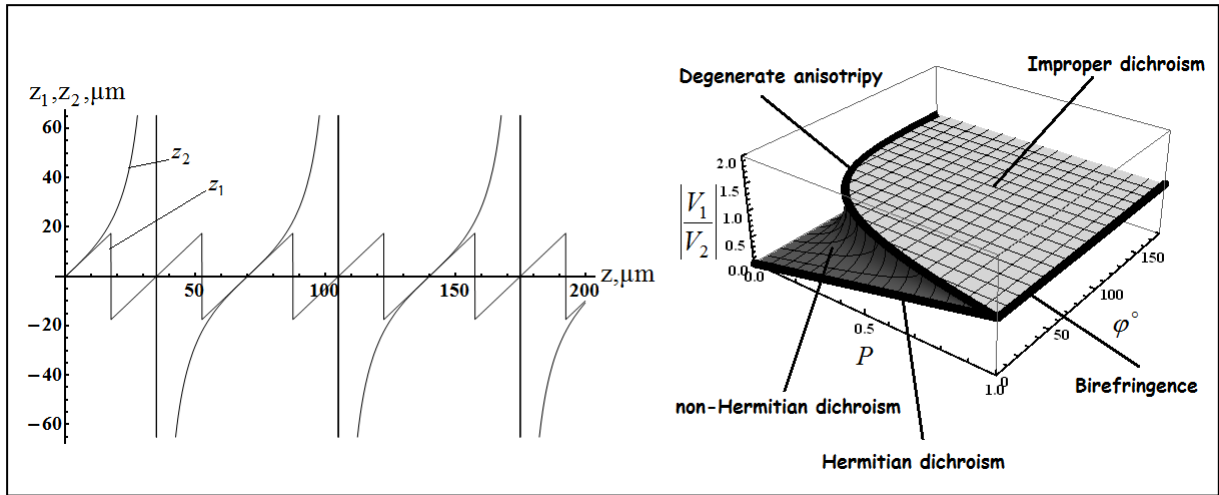


Fig. 1: Some features of first (left; Quartz,  $\lambda = 632nm$ ) and second (right) Jones equivalence theorems

For the first Jones equivalence theorem, Fig.1 presents the dependence of “simultaneous” path length  $z$  on partial path lengths  $z_1$  and  $z_2$  in accordance with the relation:

$$\mathbf{T}^{EP}(\delta, \varphi, \alpha_1, z) = \mathbf{T}^{LP}(\delta, \alpha_2, z_1) \mathbf{T}^{CP}(\varphi, z_2), \quad (1)$$

where superscripts  $EP$ ,  $LP$ , and  $CP$  denote elliptical, linear and circular birefringence, respectively;  $\delta$  and  $\alpha_i$  - value and azimuths of linear birefringence;  $\varphi$  - value of circular birefringence.

For second Jones equivalence theorem, Fig. 1 presents the dependence of absolute value of eigenvalues ratio on values of linear dichroism  $P$  and circular birefringence  $\varphi$ . It can be seen that in contrast to the case of the generalized equivalence theorem decomposition [4] this dependence is asymmetric with respect to the plane  $\varphi = 90^\circ$ .

- [1]. S. Kumar, H. Purwar, R. Ossikovski, A. Vitkin, and N. Ghosh, J. Biomed. Opt. **17**(10), 105006 (2012)
- [2]. S. Savenkov, V. Marienko, E. Oberemok, and O. Sydoruk, Phys Rev E **74**, 056607 (2006).
- [3]. H. Hurwitz, C. Jones, J. Opt. Soc. Am., **31**, 493-499 (1941).
- [4]. S. Savenkov, O. Sydoruk, R. Muttiah, Appl. Opt., **46**(27), 6700-6709 (2007).

## METHOD FOR SMALL ELLIPTICITIES MESUREMENT OF COHERENT LIGHT

Evelina BIBIKOVA<sup>1,2</sup>, Nataliya KUNDIKOVA\*<sup>1,2</sup>

<sup>1</sup>*South Ural State University, 76 Lenin Av., Chelyabinsk, Russia;*

<sup>2</sup>*Institute of Electrophysics of UD RAS, 106 Amundsen St., Yekaterinburg, Russia*

Keywords: polarization, coherence, retardation, ellipticity

Linear polarized light can acquire ellipticity due to reflection from thin films, due to vacuum magnetic birefringence. Elliptical polarization appears in localized structures in broad area vertical-cavity surface-emitting lasers or due to strong interaction between chiral molecules and orbital angular momentum of light. To determine the ellipticity of a light beam, photometric methods comprising the Stokes parameters measurement and compensation methods are used. In principle, the known photometric methods make it possible to measure small ellipticities, but require precision photometric instruments and rather powerful lasers. Compensation methods require a retardation plate and a polarizer. If elliptically polarized light propagates through the compensator and the polarizer, light extinction can occur under proper orientation of the compensator and the polarizer. To determine any state of polarization, a quarter wave plate with a phase retardation  $\Gamma = \pi/2$  is usually used.

Here we propose a new ellipsometric method for the investigation of coherent light with small ellipticity. The principal feature of this method is the use of a compensator with small retardation and taking into account multiray interference of coherent light [1].

The compensator with a retardation of  $\Gamma_c = 1^\circ$  was made from two mica plates according to the method described in [1,2]. The measured relative error of ellipticity  $\Delta e/e$  as a function of ellipticity itself  $e$  is shown in Fig. 1. Figure 1 shows that the value of  $\Delta e/e$  does not exceed 2 % for the range of  $8 \times 10^{-4} \div 5 \times 10^{-3}$ . The error greatly increases in the ellipticities range of  $3 \times 10^{-4} \div 8 \times 10^{-4}$ .

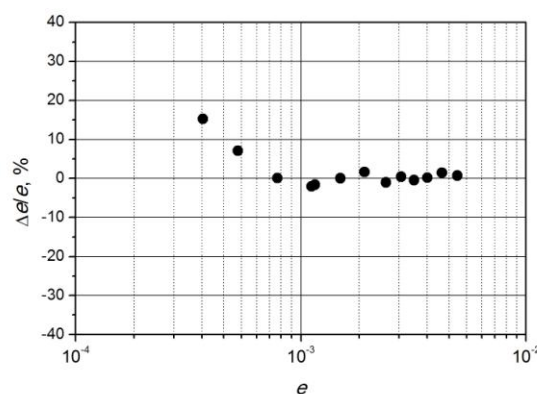


Fig. 1: The measured relative error of ellipticity  $\Delta e/e$  as a function of the value of ellipticity  $e$

This work was partly carried out within the scope of the topic of State Assignment No. 0389-2014-0030.

[1]. E.A. Bibikova, N.D. Kundikova, *Appl. Opt.*, **52**, 1852–1856 (2013)

[2]. I. Goltser, M. Darscht, N. Kundikova, B. Zel'dovich, *Optics Commun.*, **97**, 291–294 (1993)

## **Illumination spectral bandwidth as a new degree of freedom for active polarimetric imagers in target detection applications**

Lijo Thomas,<sup>1</sup> Matthieu Boffety,<sup>1</sup> François Goudail\*,<sup>1</sup>

<sup>1</sup>*Laboratoire Charles Fabry, Institut d'Optique Graduate school,  
2, Augustin Fresnel, Palaiseau, France*

Keywords: optics, polarization.

Polarization imaging is a technique which reveals contrasts that do not appear in classical intensity images. It transforms the difference in polarimetric properties of a scene into difference in gray level of an image. This technique has found applications in decamouflaging, remote sensing, microscopy etc. Polarimetric imagers often use polarization modulation devices based on liquid crystal variable retarders (LCVR), which are fast and reliable. However, LCVR control the polarization state of light only at one given nominal wavelength, and performance loss might be observed if imaging is performed at other wavelengths, due to the wavelength dependence of the LCVR. If the light source that illuminates the scene has a broad spectrum (for example, a white light source), it is thus necessary to insert a narrowband spectral filter in the imaging path. However, spectral filtering significantly decreases the amount of light entering the system and thus the signal-to-noise ratio of polarimetric images.

A way to circumvent this issue is to achromatize the polarization modulators. However, this comes at the price of higher complexity and cost, and this may not be needed if the objective is to improve target detection performance by increasing the target/background discriminability (or contrast). In our poster, we present the investigation of the impact of broadening the spectrum of the light entering the system on the discriminability performance of active polarimetric systems. Through simulations, we show that broadening the bandwidth of the illumination can increase the contrast between two regions, as the increase of light flux compensates for the loss of polarimetric precision. Moreover, we show that taking into account the chromatic characteristics of the components of the imaging system, it is possible to further enhance the contrast. We validate these findings through experiments in active polarimetric imaging configuration, and demonstrate that the spectral bandwidth can be considered as an additional parameter to optimize polarimetric imaging set-ups.

[1]. M. Boffety, H. Hu, and F. Goudail, *Opt. Lett.* 39, 6759–6762 (2014).

[2]. L.Thomas, M.Boffety and F.Goudail, *Opt. Express* 23, 33514-33528 (2015).

[3]. L.Thomas, M.Boffety and F.Goudail, *Proc. SPIE* 9853, 98530K (2016).

## **DETECTION OF CERVICAL NEOPLASIA USING MUELLER POLARIMETRIC IMAGING: CONTINUED STATISTICAL EVALUATION**

Meredith KUPINSKI<sup>1</sup>, Jean REHBINDER<sup>2</sup>, Huda HADDAD<sup>3</sup>, Stanislas DEBY<sup>2</sup>, Jérémy VIZET<sup>2</sup>, Benjamin TEIG<sup>4</sup>, André NAZAC<sup>5,6</sup>, Angelo PIERANGELO<sup>2</sup>, François MOREAU<sup>2</sup>, Tatiana NOVIKOVA<sup>2</sup>

<sup>1</sup>*University of Arizona, Tucson, Arizona, USA*

<sup>2</sup>*LPICM, Ecole polytechnique, CNRS, Palaiseau 91128, France*

<sup>3</sup>*Applied physics department, Faculty of science, Tafila Technical University, Tafila, Jordan*

<sup>4</sup>*CHU de Bicêtre, Service d'anatomie pathologique, Le Kremlin-Bicêtre 94270, France*

<sup>5</sup>*Service de Gynécologie Obstétrique, CHU de Bicêtre AP-HP, Le Kremlin-Bicêtre 94275, France*

<sup>6</sup>*Department of Obstetrics and Gynecology, University Hospital Brugmann, Université Libre de Bruxelles, Brussels, Belgium*

Keywords: Mueller polarimetry, cervical cancer, statistical decision theory

A prior proof-of-concept study demonstrated significant contrast in Mueller polarimetric images acquired for healthy and pre-cancerous regions of excised fixed cervical tissue [1]. To quantify the ability of this technique to differentiate between healthy and pre-cancerous tissue, polarimetric Mueller images of seventeen cervical specimens were compared to results from histopathology. The sensitivity and specificity of the new polarimetric technique were calculated for images acquired at wavelengths of 450nm, 550nm, and 600nm, aiming to differentiate between high-grade cervical intraepithelial neoplasia (CIN 2-3) and healthy squamous epithelium. An optimized value of ~83% was achieved for both sensitivity and specificity for images acquired at 450nm and for a threshold scalar retardance value of  $10.6^\circ$ . In this work we aim to improve the sensitivity and specificity of polarimetric cervical cancer detection by using novel detection algorithms designed to compute quadratic classifiers from high-dimensional image data [2]. This J-optimal channelized quadratic observer (J-CQO) is an algorithm that can incorporate all polarimetric, spectral, and local spatial measurements into the classifier. These measurements are linearly combined; the novelty of the algorithm is computing the linear transform that is optimal for the detection task by using a non-linear manifold optimization. We will report variability in the sensitivity and specificity of Mueller polarimetric imaging as a function of spectral, polarimetric, and spatial sampling. This analysis allows an interpretation of the utility of each measurement with respect to the detection of cervical cancer. Evaluating the utility of the high-dimensional Mueller spectra-polarimetric image measurements will serve to improve this novel modality for cervical cancer detection.

The area under the receiver operating characteristic curve (ROC) is computed to quantify J-CQO performance. The 17 patients are divided into three non-overlapping groups: patient data to solve for the optimal linear transform, patient data to train the quadratic classifier, and patient data to test the performance of the J-CQO classifier. Patient variability is a large source of uncertainty in the classifier; the AUC depends strongly on which three non-overlapping groups are selected and the quantity of patients divided into each group. The AUC ranges from 0.98 to 0.72 depending upon the group selection.

- [1]. Rehbinder J, Haddad H, Deby S, et al; Ex vivo Mueller polarimetric imaging of the uterine cervix: a first statistical evaluation. *J. Biomed. Opt.* 0001;21(7):071113. doi:10.1117/1.JBO.21.7.071113.
- [2]. M. K. Kupinski and E. Clarkson, "Method for optimizing channelized quadratic observers for binary classification of large-dimensional image datasets," *J. Opt. Soc. Am. A* 32, 549-565 (2015).

## **MUELLER POLARIMETRIC IMAGING OF UTERINE CERVIX: FROM PROOF OF PRINCIPLE EXPERIMENTS TO *IN VIVO* MEASUREMENTS**

Jean REHBINDER<sup>1</sup>, Jérémy VIZET<sup>1</sup>, Stanislas DEBY<sup>1</sup>, Stéphane ROUSSEL<sup>1</sup>, Tatiana NOVIKOVA<sup>1</sup>, André NAZAC<sup>2,3</sup>, Ranya SOUFAN<sup>4</sup>, Catherine GENESTIE<sup>4</sup>, Christine HAIE-MEDER<sup>5</sup>, Anne-Gaëlle POURCELOT<sup>2</sup>, Perrine CAPMAS<sup>2</sup>, Sylvie ZANON<sup>2</sup>, Hervé FERNANDEZ<sup>2</sup>, François MOREAU<sup>1</sup>, Angelo PIERANGELO<sup>1</sup>

<sup>1</sup>*LPICM, Ecole polytechnique, CNRS, Palaiseau 91128, France*

<sup>2</sup>*Service de Gynécologie Obstétrique, CHU de Bicêtre AP-HP, Le Kremlin-Bicêtre 94275, France*

<sup>3</sup>*Department of Obstetrics and Gynecology, University Hospital Brugmann, Université Libre de Bruxelles, Brussels, Belgium*

<sup>4</sup>*Institut Gustave Roussy, Service d'anatomie pathologique gynécologique, Villejuif 94800, France*

<sup>5</sup>*Institut Gustave Roussy, Département de Curiothérapie, Villejuif 94800, France*

Keywords: cervical cancer, polarimetry, tissue anisotropy, colposcopy

Nowadays cervical cancer continues to be a major health issue causing the death of 275000 women per year worldwide. Polarimetric imaging is a potential alternative to the standard screening methods currently used in clinics. Accordingly, polarimetric imaging of the uterine cervix has attracted a lot of attention in the last few years. Preliminary *ex vivo* results on fresh conization specimens [1] showed that healthy tissues are characterized by a strong anisotropy which is considered to be the signature of the structured and ordered collagen composing the connective tissue beneath the epithelium. Pre-cancerous changes in the epithelium can degrade the structure of collagen fibers in the nearby connective tissue, with the consequence of decrease in its macroscopically measurable anisotropy. These preliminary results have been quantitatively evaluated in a recent study comparing Mueller polarimetric images to histological analysis [2]. Currently *in vivo* measurements in hospital settings are being performed in the perspective of future use in clinical practice.

- [1]. A. Pierangelo et al "Polarimetric imaging of uterine cervix: a case study" Opt. Express. 21(12):14120-30 (2013)
- [2]. J. Rehbinder et al "Ex vivo Mueller polarimetric imaging of the uterine cervix: a first statistical evaluation" J. Biomed. Opt. 0001;21(7):071113 (2016) doi:10.1117/1.JBO.21.7.071113.

## **AUTOFLUORESCENCE POLARIZATION SPECTROSCOPY FOR DIFFERENTIATION BETWEEN CANCEROUS AND NORMAL COLORECTAL TISSUES**

Tsanislava GENOVA\*,<sup>1</sup> Ekaterina BORISOVA,<sup>1</sup> Nikolai PENKOV,<sup>2</sup> Borislav VLADIMIROV,<sup>2</sup> Latchezar AVRAMOV,<sup>1</sup>

<sup>1</sup>*Institute of Electronics, Bulgarian Academy of Sciences, 72, Tsarigradsko Chaussee Blvd., 1784 Sofia, Bulgaria;*

<sup>2</sup>*Queen Jovanna-ISUL University Hospital, 8, Bialo More str., 1527 Sofia, Bulgaria*

**Keywords:** synchronous fluorescence spectroscopy, polarization fluorescence spectroscopy, colon cancer

The wide spread of colorectal cancer and high mortality rate among the patients, brings it to a level of high public health concern. Implementation of standard endoscopic surveillance proves to be effective for reduction of colorectal cancer patients' mortality, since its early diagnosis allows eradication of the disease prior to invasive cancer development, but it is insufficient for further improvement. Therefore the development of complimentary diagnostic techniques of the standard white-light endoscopy is on high demand. The non-invasive and highly informative nature of the fluorescence spectroscopy brings it out as one of the most realistic prospects of an add-on "red flag" technique for early endoscopy detection of colorectal cancer. However in order for the fluorescence spectroscopy to reach its full potential as a cancer diagnostic technique further investigations are necessary.

In order to work in this direction we apply synchronous fluorescence spectroscopy (SFS), which is a steady-state approach for fluorescence spectroscopy measurements with superior sensitivity, in our investigations for evaluation of specific fluorescence characteristics of cancerous colorectal tissues. The reported results for the feasibility of polarization fluorescence technique to enhance the contrast between normal and cancerous tissues prompt us to combine it with the SFS approach. Thus additional linear polarization elements were used on the way of the excitation and emission fluorescence light beams. The polarization effects were investigated in parallel and perpendicular linear polarization modes respectively. The excitation applied was in the region of 280 - 440 nm, with 1 nm scanning step, and offset in the range of 10-200 nm with increment of 10 nm. The investigated samples are pairs of healthy and cancerous ex vivo colorectal tissue samples, which are excised during standard surgical procedures for tumour removal carried out in University Hospital "Queen Jovanna"-ISUL. Directly after the excision the tissue is immersed in safe-keeping solution, transported in isothermal conditions to the spectroscopic laboratory and the measurements were performed, as soon as possible after the excision. All patients received and signed written informed consent and this research is approved by the Ethics Committee of the University Hospital "Queen Jovanna"-ISUL.

Our previous experience with SFS technique showed its great potential for accurate, highly sensitive and specific discrimination between cancerous and normal colorectal tissue. Since one of the major sources of endogenous fluorescence with diagnostic meaning is the structural protein – collagen, which is characterized with high anisotropy, we've expected and observed an enhancement of the spectral differences between cancerous and normal colorectal tissue, which could be beneficial for the colorectal tumour' diagnostics using SFS.

## Variation of polarimetric properties of isotropic and anisotropic scattering samples with thickness within the framework of differential Mueller matrix formalism

Sang Hyuk YOO<sup>1</sup>, Tatiana NOVIKOVA<sup>1</sup>, Enric GARCIA-CAUREL<sup>1</sup>, Alexander BYKOV<sup>2</sup>, Alexey POPOV<sup>2</sup>, Igor MEGLINSKI<sup>2</sup>, Razvigor OSSIKOVSKI<sup>1</sup>

<sup>1</sup>LPICM, CNRS, Ecole Polytechnique, Université Paris-Saclay, 91128 Palaiseau, France;

<sup>2</sup>Optoelectronics and Measurement Techniques Laboratory, University of Oulu, P.O. Box 4500, 90014 Oulu, Finland

Keywords: Mueller matrix polarimetry; differential decomposition; complex scattering media

In general, natural and manmade scattering media exhibit both depolarizing and polarizing properties. In such media, the depolarization and polarization properties not only manifest themselves simultaneously in an entwined fashion, but they also evolve differently with the increase of the path-length of transmitted light. Transmission Mueller polarimetry, combined with Mueller matrix differential decomposition, appear to be well adapted experimental and analysis tools for the characterization of the polarimetric properties of complex scattering media. We report on the results of using this combined approach to study the thickness dependence of the depolarization and polarization properties of solid isotropic and anisotropic turbid media. The special focus on polarimetric properties of anisotropic turbid media is of great importance for the polarimetric studies of more complex biological structures found in histological slides of tissues used for biomedical diagnosis.

We fabricated different phantom tissues using (i) TiO<sub>2</sub> particles embedded in a transparent polymer matrix which exhibit isotropic depolarization, (ii) glassy plastic tape, which exhibit strong linear birefringence and depolarization. The phantom samples were measured with an innovative in-house Mueller matrix microscope which produces polarimetric images in both, real and reciprocal momentum (Fourier) space. Real space images allow measuring the spatial distribution of the polarimetric response of the sample, whereas Fourier space images allow measuring the angular distribution of the intensity and polarization of light scattered by the sample. Fourier space images in combination with Monte Carlo simulations can be used to interpret the influence of multiple scattering on the degree of polarization of light measured in real space images. All studied structural combinations were properly analyzed using differential decomposition of measured Mueller matrices. In particular, we found that the depolarizing and polarizing properties of the studied media evolve parabolically and linearly, respectively, with the sample thickness (see Fig. 1), in agreement with the fluctuating homogeneous medium model [1]. The reported results are of special interest for biomedical applications of transmission Mueller matrix polarimetry, such as optical biopsy for the early cancer detection.

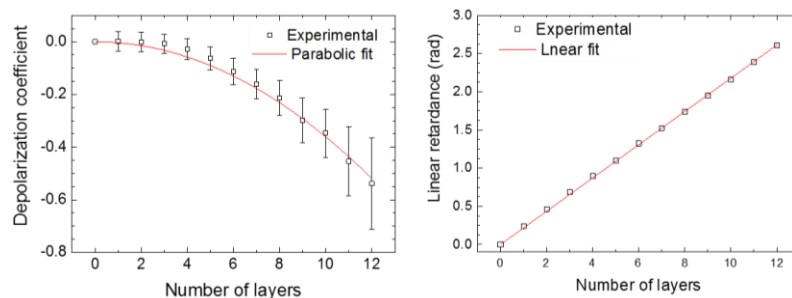


Fig. 1: Experimental diagonal depolarization coefficients (left) and linear retardance (right) of glassy tapes as function of the normalized sample thickness.

[1]. R. Ossikovski and O. Arteaga, *Opt. Lett.*, **39**, 4470-4473 (2014)

## **MULTIFUNCTIONAL POLARIZATION-CORRELATION MICROSCOPY AND LASER AUTOFLUORESCENCE POLARIMETRY OF OPTICAL ANISOTROPIC BIOLOGICAL LAYERS**

Oleg V. ANGELSKY<sup>1</sup>, Alexander G. USHENKO<sup>1</sup>, Alexander V. DUBOLAZOV<sup>1</sup>,  
Yuriy A. USHENKO<sup>1</sup>

<sup>1</sup>*Correlation Optics Department, Chernivtsi National University, Chernivtsi 58012, Ukraine;*

Keywords: polarimetry, autofluorescence, optical anisotropy

The investigation is devoted to the determination of multiparametric interconnection between the set of statistic, correlation and fractal parameters, which describe the azimuthally-independent distributions of values of polarization, phase, Mueller-matrix, polarization-correlation maps of microscopic and molecular images of histological sections of biological tissues and fluids, and the distributions of parameters of linear and circular birefringence of polycrystalline networks of such optical anisotropic layers. For analysis and description of optical anisotropy of biological layers it have been proposed the azimuthally-independent Mueller-matrix invariants that allowed to find the interconnection between the set of statistic, correlation and fractal parameters, which characterize the distributions of values of polarization, phase and vector-parametric images of polycrystalline networks, and the changes of distributions of their linear and circular birefringence. The mueller-matrix model of description of laser autofluorescence of birefringent networks of optically active complexes of biological tissues and fluids has been elaborated. The Mueller-matrix invariants of laser autofluorescence, which characterize the polarization manifestations of fluorescence of "linear" and "elliptical" oscillators on the background of linear birefringence and optical activity of proteins of biological layers have been determined.

## Chiroptical properties photo-induced by femtosecond laser irradiation in silica glass

Jing TIAN,<sup>1</sup> Rudy DESMARCHELIER,<sup>2</sup> Matthieu LANCERY,<sup>1</sup> Bertrand POUMELLEC,<sup>1</sup>

<sup>1</sup> ICMMO-SP2M, CNRS-UPSud, Université Paris Sud in Université Paris Saclay, Bâtiment 410, 91405 Orsay, France

Keywords: Lasers and laser optics; silica glass; chiral optical properties

Femtosecond laser pulses focusing in silica are absorbed through nonlinear photoionization mechanisms, which induce 3D localized modifications in silica depending on the laser parameters such as refractive index changes, nanostructuring or voids [1]. Applications are numerous in a large number of domains for health, optical storage, microfluidics and optical components like 3D optical waveguides and fiber Bragg gratings [2]. If one proves to be able to control these modifications, one could exceed the current applications of the lasers and open new possibilities in materials sciences. In 2003, we revealed that femtosecond laser interaction can shear matter like a scissor giving rise to a chiral strain if we take into account the light propagation axis. In the present work, we demonstrate that laser-matter interaction can imprint circular optical properties with such efficiency that the reciprocity of the light propagation in the glass is broken. More clearly, we show that in the case of inhomogeneous sample combining linear and circular optical properties, the light propagation is no more reciprocal. Estimates of circular dichroism show values close to what it is found for organic molecules that is sufficient to think about devices based on chiral assemblies of metal nanoparticles. We can suggest that the breaking of symmetry arises from a volume torque due to the combined action of stress field and a DC electric field (defined by the pulse front tilt and the laser polarization).

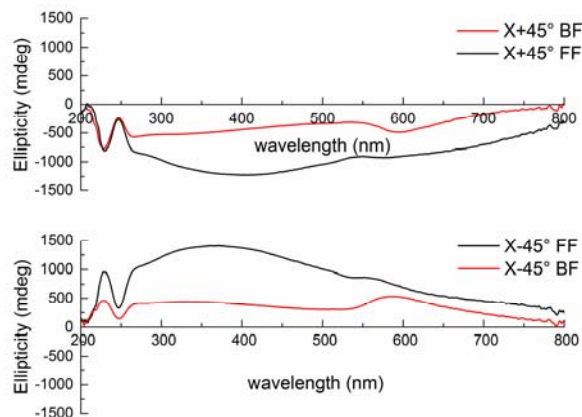


Fig. 1: Ellipticity according wavelength for both face (FF) and the back face (BF) for X+45° and X-45° writing configurations. Laser writing conditions: 1030 nm, 250 fs, 100 kHz, 0.6 NA, writing speed: 1mm/s, 1.5μJ/pulse

This new functionalization process could provide a platform for a versatile new class of photonic devices. In biomimetic fashion, we can imagine to produce cholesteric liquid crystal analogous optical devices using tiny lengths of inorganic glass i.e. "twisted silica glass" rather than a macroscopic assembly. An example could be the production of chiral devices that can be harnessed for producing sensors, polarizers, optical isolators, and filter/lasers. The femtosecond laser offers thus here a new advantage, partly in a non-conventional way: it allows restructuring of our most important optical material, to enable chirality and rotating power.

- [1]. Poumellec, B., et al., Modification thresholds in femtosecond laser processing of pure silica: review of dependencies on laser parameters [Invited]. *Optical Materials Express*, 2011. **1**(4): p. 766-782.
- [2]. Beresna, M., M. Gecevičius, and P.G. Kazansky, Ultrafast laser direct writing and nanostructuring in transparent materials. *Advances in Optics and Photonics*, 2014. **6**(3): p. 293-339.

## **Micro-waveplates and space variant birefringent optical components photo-induced by femtosecond laser**

Matthieu Lancry\*,<sup>1</sup> Jing Tian,<sup>1</sup> and Bertrand Pommellec<sup>1</sup>

<sup>1</sup>*Institut de Chimie Moléculaire et des Matériaux d'Orsay, UMR CNRS-PSUD 8182, Université de Paris Sud, Bât.410, 91405 Orsay, France*

Keywords: laser processing, laser-induced birefringence, space variant birefringence, polarization

Current advanced femtosecond laser systems offer a myriad of possibilities to modify glassy media: from surface ablation, annealing, voids to 3D refractive index modification (positive or negative index change with isotropic or anisotropic properties) depending on the laser parameters. Recently, new unique properties of laser induced glass modifications have been discovered including chirality, directional dependent writing, glass decomposition and elemental distribution with a sub-wavelength resolution. To our knowledge, no other technique holds the same potential to realize 3D multi-functional photonic devices, fabricated in a single step in a wide variety of transparent materials, particularly high temperature silica. In particular self-assembled nanogratings, which are composed of nanoporous silica regions with a low refractive index, lead to a strong negative ( $-10^{-2}$ ) form birefringence with the slow axis oriented perpendicular to the polarization of the laser beam. As a result, the retardance values exceeding 250 nm (i.e. half-wave for 532 nm YAG laser) can be readily achieved within a 30  $\mu\text{m}$  thick single layer with well-defined control of the optical axis. During the past few years, a growing number of applications based on these porous nanogratings have been demonstrated. Recent achievements include 5D optical data storage, space-variant polarization converters branded as the S-waveplates, optical retarders for integrated optics.

These nanostructures can be accumulated along the propagation direction with sub-micrometer control. These can be used as the building blocks for novel optical elements based on highly precise and strong accumulated retardance when needed. The developed multiple order waveplates open the door to Z-spatially birefringent element fabrication (a silica analog of a twisted nematic liquid crystals where there is a constant value of retardance with the continuously varying direction of the slow axis in the z direction). These silica waveplates exhibit enormous advantages including a broad spectral range from UV to IR, high thermal stability (no decay after 2 hours at 1000°C). This is primarily due to the intrinsic structures (nanoporous silica) and the absence of glued components found in some commercial waveplates, and a much higher damage threshold ( $25 \pm 3 \text{ J/cm}^2$ , at  $\lambda = 1064 \text{ nm}$ , 3.5ns, 10Hz). The major remaining problem is the significant light scattering, which introduces large losses in the UV range, which can partly be reduced by mastering the silica glass decomposition process.

Recently by replicating twisted nematic liquid crystals design we have developed a prototype of achromatic polarization rotator operating over a broadband spectral range of 600 - 1600 nm. The rotators are directly imprinted by a femtosecond laser into silica glass. The achromatic rotator offers constant retardance over a broad spectral range from VIS to NIR, integration within the bulk of transparent material, which eliminates a need for optically cemented layers and complex assembly procedures. The spectral range can be further extended in the mid-IR by cumulating higher retardance. The viable operation in the UV range requires significant reduction of scattering associated with the nanoporous oxide formed in the nanogratings. Potentially this technology can be exploited for demonstration of other useful optical components such as achromatic depolarizers, achromatic polarization converters or achromatic micro-waveplates arrays for microscopy, spectroscopy and polarimetry imaging.

## **ASSESSMENT AND MODELING OF ANISOTROPIC BIOLOGICAL TISSUE WITH MUELLER MATRIX POLARIMETRY**

Jessica C. RAMELLA-ROMAN,

<sup>1</sup>*Department of Biomedical Engineering  
Florida International University, Miami, Florida, USA;*

<sup>2</sup>*Department of Cellular Biology and Pharmacology*

<sup>3</sup>*Department of Ophthalmology  
Herbert Wertheim College of Medicine  
Florida International University, Miami, Florida, USA;*

Keywords: optics, polarization, Mueller Matrix Polarimetry, Monte Carlo

The extra-cellular space in connective tissue of animals and humans alike is comprised in large part of anisotropic structures. For example collagen is one of such dominating structure whose arrangement and cross-linking has been utilized to diagnose medical conditions and guide surgical intervention.

We have developed a suite of tools and models based on polarized aimed at the assessment of birefringence and orientation of anisotropic media, including collagen, in living tissues. Here we will present some examples of such approach to different biomedical applications.

We will show our engineering strategies in the development of Mueller Matrix polarimeters for clinical imagery, as well as illustrate our utilization of Monte Carlo[1, 2] models of polarized light transfer in the assessment of extracellular matrix remodeling typical of some pathological conditions.

1. Ghassemi, P., et al., *A new approach for optical assessment of directional anisotropy in turbid media*. J Biophotonics, 2016. **9**(1-2): p. 100-8.
2. Ramella-Roman, J., S. Prah, and S. Jacques, *Three Monte Carlo programs of polarized light transport into scattering media: part I*. Opt Express, 2005. **13**(12): p. 4420-38.

## **POLARIZATION-RESOLVED SECOND HARMONIC IMAGING OF COLLAGEN-RICH TISSUES**

Claire TEULON<sup>1</sup>, Gaël LATOUR<sup>1,2</sup>, Guillaume DUCOURTHIAL<sup>1</sup>, Ivan GUSACHENKO<sup>1</sup>,  
Marie-Claire SCHANNE-KLEIN<sup>1</sup>

<sup>1</sup> *Laboratoire d'Optique et Biosciences, Ecole Polytechnique, CNRS, INSERM, Université Paris-Saclay, Palaiseau, France;*

<sup>2</sup> *Laboratoire Imagerie et Modélisation en Neurobiologie et Cancérologie, Univ. Paris-Sud, CNRS, Université Paris-Saclay, Orsay, France*

Keywords: optics, polarization, Second Harmonic Generation, biological tissues

Collagen is the main component of connective tissues, including skin, cornea, bone, arteries... and is responsible for their biophysical and mechanical properties. This structural protein is synthesized as a triple helix, which self-assembles into fibrils (10-300 nm diameter) and further forms various 3D organizations specific to each tissue. In situ 3D visualization of this biopolymer is therefore a major biomedical concern in order to probe its accumulation or disorganization in many diseases, or to guide the engineering of tissue substitutes with a suitable 3D organization.

Second harmonic generation (SHG) microscopy has proved to be a powerful technique for the visualization of fibrillar collagen. It offers high specificity and unequalled contrast, without any prior labeling, which is not possible using conventional imaging techniques. Further information about the 3D organization of collagen can be gained with polarization-resolved second harmonic generation (P-SHG) microscopy. Two quantitative structural parameters are measured by rotating the polarization of the exciting laser beam: mean in-plane orientation of collagen molecules in the excitation volume (0.350 x 0.350 x 1.0  $\mu\text{m}^3$ ) and SHG signal anisotropy that is the ratio of SHG signal for parallel versus perpendicular orientation of the excitation polarization to the collagen main direction. The latter parameter is related to the molecular structure of collagen and to its 3D distribution inside the excitation volume at submicrometric scale: it increases with the orientation disorder and with the out-of-plane orientation angle [1, 2].

In this talk, we first discuss the accuracy and reliability of P-SHG measurements. We mostly characterize the effect of strong focusing and derive experimental conditions enabling reproducible measurements [3]. We then present results obtained by P-SHG analysis in various collagen-rich tissues or model systems. First, we show that P-SHG can monitor the increase of the alignment of collagen fibrils in a tendon subjected to controlled mechanical stretching [1]. Second, we illustrate the sensitivity of P-SHG microscopy to anisotropic structures at sub-micrometer scale by imaging corneas that are composed of stacked lamellae containing aligned fibrils with 30 nm diameter: we show that P-SHG images reveals the direction of these collagen fibrils while they are not resolved in the SHG images [4]. Finally, we use P-SHG microscopy to characterize collagen liquid-crystal structures similar to those found as stabilized structures in cornea or bone. We demonstrate the benefits of P-SHG microscopy to quantify the phase transitions and decipher their 3D structure, in particular the out-of-plane orientation of collagen molecules [2].

All these experimental results prove the efficiency of P-SHG microscopy for in situ characterization of the 3D distribution of collagen in tissues or synthetic structures.

[1]. I. Gusachenko, Y. Goulam Houssen, V. Tran, J.M. Allain, M.C. Schanne-Klein, *Biophys J* 102, 2220 (2012)

[2]. C. Teulon, A. Tidu, F. Portier, G. Mosser and M.-C. Schanne-Klein, *Opt. Express* 24, 16084 (2016)

[3]. C. Teulon, I. Gusachenko, G. Latour, and M.-C. Schanne-Klein, *Opt. Express* 23, 9313-9328 (2015)

[4]. G. Latour, I. Gusachenko, L. Kowalczyk, I. Lamarre, M.C. Schanne-Klein, *Biomed Opt Express* 3, 1 (2012)

## PROBING BIOLOGICAL TISSUES WITH ELLIPTICALLY POLARIZED LIGHT

Anabela DA SILVA,\* Susmita SRIDHAR, Callum MACDONALD

<sup>1</sup> Aix-Marseille Université, CNRS, Centrale Marseille, Institut Fresnel, UMR 7249,  
13013 Marseille, France;

Keywords: biomedical optics, polarization gating, elliptically polarized light

2D Intrinsic Optical Imaging (IOI) is an essential tool for non invasive screening of biological tissues. It allows obtaining high resolution 2D images, with functional in so far as spatial variations of the absorption of elementary chromophores (e.g. oxy- and deoxy- hemoglobin, glucose). The technique is widely used in neurosciences (cortex imaging [1]), ophthalmology (retina), or oncology (detection/monitoring of skin, uterus cancers...). Conventional IOI systems also offer the possibility of a dynamic monitoring, by monitoring the time variations of the absorption of the chromophores of interest in response to stimuli (visual, physical, etc.). However, the images obtained are a combination of backscattered signals coming from both surface and different sub-surface layers, and do not carry information in depth. These imaging systems suffer from i) a blurring due to specular reflections; ii) a loss of information on the origin of the measured signal, because light is collected without any discrimination on its path. Getting rid of the first problem can be obtained by using linear polarizers under cross-linear configuration. Light collected is then supposed to come from deep layers, without any further information in depth though.

Polarization gating is a unique tool that allows a filtering of light with respect to its state of polarization along its path through the probed tissue. Intuitively, polarized light will keep its original polarization up to a certain pathlength depending on the scattering mean free path that is the number of scattering events met during its travel through the tissue. The approach we use is based on the fact that circularly polarized light is maintained for a larger number of scattering events in scattering media composed of Mie scatterers (large particles), which is the case for most of biological tissues [2,3]. This maximal depth depends on the optical properties of the tissues (absorption and scattering) [4]. Furthermore, it has been shown that this depth can be tuned, between surface up to this maximum depth, as a function of the ellipticity of the polarization gate. This principle will be illustrated with theoretical [4] and experimental studies [5,6].

- [1]. Shtoyerman E., Arieli A., Slovin H., Vanzetta I., and Grinvald A., "Long-Term Optical Imaging and Spectroscopy Reveal Mechanisms Underlying the Intrinsic Signal and Stability of Cortical Maps in V1 of Behaving Monkeys," *J. Neuroscience*, 20(21), 8111–8121, 2000.
- [2]. MacKintosh, F. C., Zhu, J. X., Pine, D. J., and Weitz, D. A., "Polarization memory of multiply scattered light," *Phys. Rev. B* 40, 9342–9345 (Nov 1989).
- [3]. Morgan, S. P. and Ridgway, M., "Polarization properties of light backscattered from a two layer scattering medium," *Optics express* 7(12), 395–402 (2000).
- [4]. Rehn, S., Planat-Chrétien, A., Berger, M., Dinten, J. M., Deumié, C., and Da Silva, A., "Depth probing of diffuse tissues controlled with elliptically polarized light," *Journal of biomedical optics* 18, 16007 (2013).
- [5]. Da Silva, A., Deumié, C., and Vanzetta, I., "Elliptically polarized light for depth resolved optical imaging," *Biomedical Optics Express* 3(11), 2907 (2012).

- [6]. Sridhar, S. and Da Silva, A., “Enhanced contrast and depth resolution in polarization imaging using elliptically polarized light,” *Journal of Biomedical Optics* (Forthcoming, 2016). Special Issue: Polarized Light for Biomedical Applications.

## LASER DIAGNOSTICS OF BIOTISSUES WITH CIRCULARLY POLARIZED LIGHT

Alexander BYKOV<sup>1,\*</sup>, Alexey POPOV<sup>1</sup>, Markus MÄKINEN<sup>2</sup>,  
Tatiana NOVIKOVA<sup>3</sup>, Igor MEGLINSKI<sup>1</sup>

<sup>1</sup>*Optoelectron. and Measur. Tech. Unit, University of Oulu, P.O. Box 4500, 90014 Oulu, Finland;*

<sup>2</sup>*Department of Pathology, University of Oulu and Oulu University Hospital;*

<sup>3</sup>*LPICM, CNRS, Ecole Polytechnique, Université Paris—Saclay, 91128 Palaiseau, France*

Keywords: optics of biotissue, circular polarization

According to the statistics, cancer is one of the leading causes of mortality in EU and around the globe, accounting for 25% of all deaths in Europe [1]. In many cases, cancer is associated with the microstructural changes of biotissues such as cell nucleus enlargement and structural reorganization. Imaging with polarized light can provide rich information about the microstructure of the samples due to the extremal sensitivity of the polarized light to their inner structure and composition. However, the linearly polarized light rapidly loses its polarization due to multiple scattering. Therefore, a system that uses linear polarized light is only suitable for probing the structure of cells at or adjacent to the surface of the tissue. Our study has shown that circularly/elliptically polarized light scattered within the tissues is highly sensitive to the presence of cancer cells and can be used for diagnostics of bulk tissue-like scattering media.

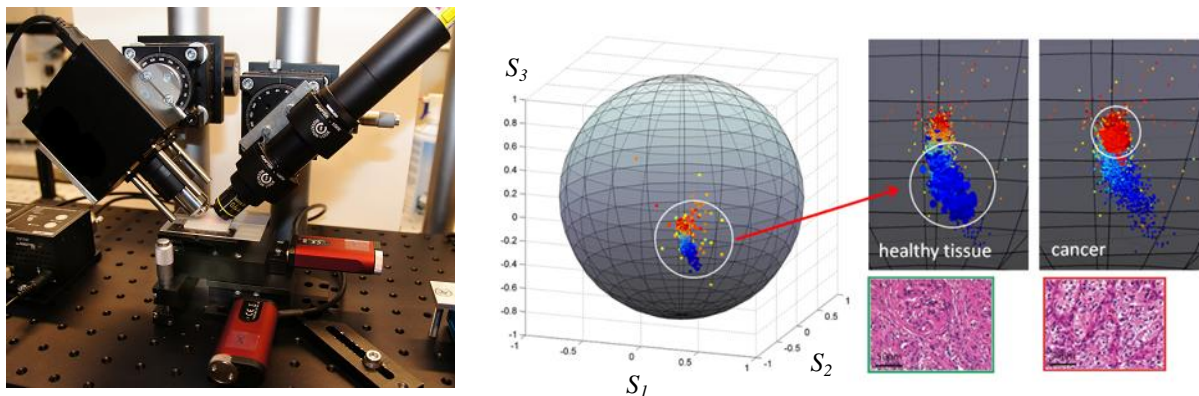


Fig.1. Photograph of the experimental setup (left). Changes of the state of polarization (Stokes vectors) of diffusely back-scattered circularly polarized light on the Poincaré sphere for cancerous (red dots) and non-cancerous (blue dots) tissues confirmed by conventional biopsy (right).

Schematic of the experimental system for noncontact diagnostics of biological tissues by using diffusely reflected circularly polarized light is presented in Fig. 1. Diffusely backscattered polarized light is collected at a distance  $d$  from the focus point and is then passed through a polarimeter to measure degree of polarization. The source-detector separation as well as the angle of detection can be varied to influence the sampling volume. Multiple measurements have been performed on a human lung metastasis of basal squamous cell carcinoma embedded in paraffin wax. These samples had a variety of tissue structures previously classified by the pathologist. To visualize and compare the polarization state of the detected radiation the Poincaré sphere was used [2]. The cancerous and healthy tissue samples have shown that their scattered polarization states are clearly distinguishable from one another. It is noticeable that the polarization state of the diffusely backscattered light from the cancerous samples is located mostly on the upper regions of the northern hemisphere, while the healthy tissues correspond to lower latitudes.

- [1]. Organisation for Economic Co-operation and Development (OECD), Health at a Glance: Europe 2015.  
[2]. B. Kunnen, et al., J. Biophoton., 8(4), 317-323 (2015).

## Polarization spatial distributions generator based on a single Parallel Aligned Liquid Crystal on Silicon Display

Irene ESTÉVEZ\*,<sup>1</sup> Angel LIZANA<sup>1</sup>, Xuejie ZHENG<sup>1</sup>, Alba PEINADO<sup>1</sup>, Claudio RAMIREZ<sup>1</sup>, Jose Luis MARTÍNEZ<sup>2</sup>, Andrés MÁRQUEZ<sup>2</sup>, Ignacio MORENO<sup>3</sup>, Juan CAMPOS<sup>1</sup>

<sup>1</sup>*Departament de Física, Universitat Autònoma de Barcelona, 08193, Bellaterra, Spain*

<sup>2</sup>*Departamento de Física, Department of Physics, Systems Engineering and Signal Theory, Universidad de Alicante, Ap. 99, 03080, Alicante, Spain*

<sup>3</sup>*Department of Materials Science, Optics and Electronics Technology, Universidad Miguel Hernández de Elche, 03202, Elche, Spain*

Keywords: vector beam, arbitrary polarization distributions, LCOS display

The generation of controlled polarization patterns is of interest in a number of different applications. For instance, cylindrical vector beams [1], among which radially and azimuthally polarized beams are particular cases, are of especial interest because of some of the properties they exhibit upon focalization with high aperture lenses, or because their relation with the orbital angular momentum of light. Additionally, they are eigen-solutions of cylindrical resonators and optical fibers. Furthermore, reflective Liquid Crystals on Silicon (LCOS) display are nowadays a mature technology widespread used in applications [2]. Due to the capability of LCOS displays to act as spatial light modulators, they can be seen in optical arrangements devised to implement structured illuminators.

By taking advantage of this modulation capability of LCOS displays, we propose an experimental set-up able to provide transversal patterns with customized state of polarization spatial distributions [3]. Unlike other proposals, we provide a compact optical arrangement that generates the controlled spatial distributions just by using a single LCOS display. This is achieved thanks to an optical module present in the system. This module allows a double reflection of the input light on two different halves of the display, and provides the required polarization plane rotation between reflections. The suitability of the system is provided by experimentally generating different spatial distributions of polarization, as axial, azimuthal or spiral linear polarization patterns.

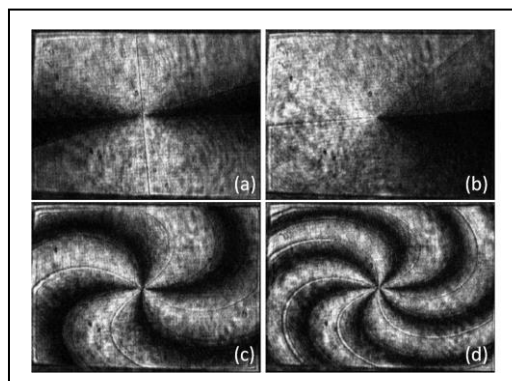


Fig. 1: Some generated polarization distributions

- [1]. Q. Zhan, *Advances in Optics and Photonics* 1, 1–57 (2009)
- [2]. Z. Zhang, Z. You, D. Chu, *Opt. Soc. Am. A, Light: Science & Applications* 3, (2014)
- [3]. X. Zheng, A. Lizana, A. Peinado, C. Ramírez, J.L. Martínez, A. Márquez, I. Moreno, *Journal of Lightwave Technology* 33(10), 2047-2055 (2015)

## TOWARDS DEPTH-RESOLVED SPECTROSCOPY USING ELLIPTICALLY POLARIZED LIGHT

Susmita SRIDHAR,<sup>1,2</sup> \* Callum MACDONALD,<sup>1</sup> Anabela DA SILVA,<sup>1</sup>

<sup>1</sup> Aix-Marseille Université, CNRS, Centrale Marseille, Institut Fresnel, UMR 7249, 13013 Marseille, France;

<sup>2</sup> ICFO – Institut de Ciències Fotoniques, Universitat Politècnica de Catalunya, 08860 Castelldefels, Barcelona, Spain

Keywords: biomedical optics, polarization gating, elliptically polarized light

Polarimetry has a long and successful history in various forms of clear media and the use of its approaches for biological tissue assessment has received considerable attention. Specifically, polarization can be used as an effective tool to discriminate against multiply scattered light (acting as a gating mechanism) in order to enhance contrast and to improve tissue-imaging resolution. However, in a complex random medium like tissue, numerous complexities due to multiple scattering and simultaneous occurrences of many scattering and polarization events present formidable challenges both in terms of accurate measurements and in terms of analysis of the tissue polarimetry signal. Biological tissues are composed of large particles compared to the wavelength (Mie Scatterers). They are known to retain their initial polarization for a larger number of scattering events in circular polarization than in linear polarization.<sup>1, 2</sup> This effect was further investigated and verified by Monte Carlo simulations in a semi-infinite medium.<sup>3</sup> It has been demonstrated that the mean visitation depth into which elliptically polarized light can penetrate is between that of linearly and circularly polarized light.<sup>4</sup> Instead of using the conventional linearly polarized illumination, we propose to take advantage of using elliptically polarized light as it allows for more selective probing in terms of depth. Co-elliptical measurements allow access to deeper subsurface volumes than collinear measurements, the depth of probing being controlled by the ellipticity of polarization. Counter-elliptical measurements attenuate subsurface signal and, hence, enhance the signal coming from deeper volumes, provided that mirror reflections are filtered. We propose a new protocol of polarization gating<sup>5</sup> data-acquisition that combines co-elliptical and counter-elliptical measurements that we call ‘Multi-Polarization Difference Imaging (MPDI)’. Validations of the approach include measurements on phantoms and *ex vivo* tissues. For the purpose of illustrating different modes of application, series of *in vivo* measurements were performed on volunteers’ skin abnormalities. Here one seeks at accessing subsurface information, co-elliptical imaging configuration is adopted in order to illustrate the selective probing in depth. In this communication, we have developed an algorithm based on the generalised form of Modified Beer-Lambert’s Law (MBLL) which revolves around a generalized theory that allows estimation of chromophore concentrations. We have adapted this theory for mapping concentrations of cutaneous tissue chromophores from multi-wavelength images that have been processed by Multi-Polarization Difference Imaging (MPDI).

[1]. MacKintosh, F. C., Zhu, J. X., Pine, D. J., and Weitz, D. A., “Polarization memory of multiply scattered light,” *Phys. Rev. B* 40, 9342–9345 (Nov 1989).

[2]. Morgan, S. P. and Ridgway, M., “Polarization properties of light backscattered from a two layer scattering medium,” *Optics express* 7(12), 395–402 (2000).

[3]. Rehn, S., Planat-Chrétien, A., Berger, M., Dinten, J. M., Deumié, C., and Da Silva, A., “Depth probing of diffuse tissues controlled with elliptically polarized light,” *Journal of biomedical optics* 18, 16007 (2013).

[4]. Da Silva, A., Deumié, C., and Vanzetta, I., “Elliptically polarized light for depth resolved optical imaging,” *Biomedical Optics Express* 3(11), 2907 (2012).

[5]. Sridhar, S. and Da Silva, A., “Enhanced contrast and depth resolution in polarization imaging using elliptically polarized light,” *Journal of Biomedical Optics* (Forthcoming, 2016). Special Issue: Polarized Light for Biomedical Applications.

## THE ALGEBRAIC DECOMPOSITION OF MUELLER MATRICES AS A TOOL FOR ENHANCED PHYSICAL INSIGHT: THEORY AND EXPERIMENT

Razvigor OSSIKOVSKI\*<sup>1</sup>, Enric GARCIA-CAUREL<sup>1</sup>, Igor MEGLINSKI<sup>2</sup>, Tatiana  
NOVIKOVA<sup>1</sup>

<sup>1</sup>*LPICM, CNRS, Ecole Polytechnique, Université de Paris - Saclay, 91128 Palaiseau*

<sup>2</sup>*University of Oulu, Oulu, Finland*

Keywords: polarization, theory of Mueller matrices

The Mueller matrix represents the most general phenomenological description of the linear interaction of an optical system or medium with polarized light. The availability of easy-to-use, fast and reliable polarimetric equipment has made possible the routine study of a wide range of complex materials and structures and has provided a large amount of data, under the form of Mueller matrices, to experimentalists. The problem of the physical interpretation of a measured Mueller matrix is, consequently, of growing importance. However, constructing a physical model for a generally depolarizing Mueller matrix is feasible, whenever possible, for a limited number of optical structures only. In the absence of a physical model describing and explaining it, an experimental Mueller matrix can still be phenomenologically interpreted by decomposing it algebraically into simpler components having a direct physical meaning. The subject of the polarimetry theory activity is the study of the properties of theoretical as well as experimental Mueller matrices by using a formal algebraic approach. The decomposition of a measured Mueller matrix into several simpler ones, representing basic polarization components (partial polarizers, wave-plates and depolarizers), often allows one to get a better insight into the physics underlying the original matrix. The decomposition approach is a purely phenomenological one, i.e. it does not require any optical modelling or simulation, but is rather based on a general principle (physical realizability condition). Related topics of significant practical interest are the determination of a non-depolarizing component out of an experimental depolarizing Mueller matrix, the best non-depolarizing estimate of a measured Mueller matrix, the best physical estimate of a measured “unphysical” Mueller matrix, the extraction of meaningful physical parameters (diattenuations, retardances, depolarization indices), the reduction of general depolarizing Mueller matrices to canonical depolarizers allowing for an objective comparison of their properties, etc.

## **CURL FORCES: NEW DYNAMICS WITH IMPLICATIONS FOR OPTICS**

Michael BERRY

*H H Wills Physics Laboratory, University of Bristol, UK*

Keywords: curl forces, optical vortices, dynamics of small dielectric particles

Forces exerted by light on small dielectric particles generally depend on position but are not derivable from a potential: their curl is non-zero. Such forces give rise to dynamics that is not Hamiltonian or Lagrangian yet non-dissipative. Noether's theorem does not apply, so the link between symmetries and conservation laws is broken. Motion under curl forces near optical vortices can be understood in detail, and numerics reveals a new kind of chaos. There are quantum implications. The full series of 'superadiabatic' correction forces is derived, leading to an exact slow manifold in which fast (internal) and slow (external) motion of the particle is separated.

## **Optical sorting of chiral entities using the angular momentum of light**

Etienne BRASSELET <sup>1,2</sup>

<sup>1</sup>*Univ. Bordeaux, LOMA, UMR 5798, F-33400 Talence, France;*

<sup>2</sup>*CNRS, LOMA, UMR 5798, F-33400 Talence, France*

Keywords: chirality, optical angular momentum, liquid crystals

Optical radiation forces and torques are the mechanical manifestation of the transfer of the linear and angular momentum of light to matter. The interplay between the chirality of matter and light allows considering several options to manipulate, in a selective manner the mechanical degrees of freedom of chiral objects depending on their chirality. This will be illustrated by a few experimental demonstrations where the optical angular momentum of light is at play [1,2,3].

[1]. G. Tkachenko and E. Brasselet, *Phys. Rev. Lett.* 111, 033605 (2013)

[2]. G. Tkachenko and E. Brasselet, *Nat. Commun.* 5, 3577 (2014)

[3]. G. Tkachenko and E. Brasselet, *Nat. Commun.* 5, 4491 (2014)

## **TRANSMISSION-MATRIX-BASED POINT-SPREAD-FUNCTION ENGINEERING THROUGH A COMPLEX MEDIUM**

Antoine BONIFACE<sup>1</sup>, Mickael MOUNAIX<sup>1</sup>, Baptiste BLOCHET<sup>1</sup>, Rafael PIESTUN<sup>1</sup>,  
Sylvain GIGAN<sup>1</sup>

<sup>1</sup> *Laboratoire Kastler Brossel, ENS, UPMC, CNRS, Collège de France, France*

Keywords: wavefront shaping, vector light beams, super-resolution imaging

When coherent light propagates through a disordered system, such as white paint or biological tissue, its spatial properties are mixed and the resulting transmitted field forms a speckle pattern. Although the size of a speckle grain is diffraction-limited, this complex interference figure is detrimental for all conventional imaging systems.

Recently, wavefront shaping techniques have opened a new way to perform imaging through disordered systems, using spatial light modulators. In particular, the optical transmission matrix (TM) links the input field to the output field. It enables arbitrary spatial focusing of light after propagation in the medium, whose size is limited by diffraction [1].

We report the first formulation of a TM-based operator that enables the focusing of arbitrary point-spread-function (PSF) after propagation in the medium [2]. We numerically compute the optical field in a virtual pupil plane by Fourier transforming the output speckle pattern. By numerically applying an arbitrary (phase and/or amplitude) mask onto this pupil, we build on this effective operator. It enables focusing of the corresponding PSF at the output of the medium.

As an example, we demonstrate the generation of Bessel beam using an amplitude annular mask, and show that the FWHM of its central peak is narrower than the size of a speckle grain. The generation of sub-diffraction pattern at the output is thus now deterministically achievable. We also excite Laguerre-Gauss beam (“donut”) using vortex masks, as well as even more complex 3D-beam profiles such as spiral PSFs, which paves the way for super-resolution imaging in turbid media.

[1] S. Popoff, G. Lerosey, R. Carminati, M. Fink, A.C. Boccara, S. Gigan, “Measuring the Transmission Matrix in Optics: An Approach to the Study and Control of Light Propagation in Disordered Media”, *Phys. Rev. Lett.* 104, 100601 (2010)

[2] A. Boniface, M. Mounaix, B. Blochet, R. Piestun, S. Gigan, “Transmission-matrix-based point-spread-function engineering through a complex medium”, arXiv:1609.00307 (2016)

## **ANGULAR MOMENTUM OF LIGHT IN BIOPHOTONIC APPLICATIONS:**

### **Usage of orbital angular momentum for ranging & super-resolved imaging and spin angular momentum for blood flow tracking & glucose sensing**

Zeev ZALEVSKY

*Faculty of Engineering and the nanotechnology center, Bar-Ilan University, Ramat Gan 52900, Israel*

**Keywords:** Optical angular momentum, Ranging, Super resolution, Biophotonics

In this presentation I will speak on how angular momentum of light can be used for some biophotonic applications. Specifically I will focus on two topics. In the first I will show how beam shaping optical elements can generate orbital angular momentum to be used for performing ranging and for improving the transversal imaging resolution. The ranging is obtained by creating axially depending rotation of a line that is rotating clockwise as the compasses of a clock and according to its angular location one may perform the ranging estimation [1]. The super resolved imaging is obtained by realizing time multiplexing structured illumination concept. However instead of projecting random patterns I will show how realization of spatial axially and temporally changing codes, similar to Barker codes, that control the orbital angular momentum of light can optimize the obtainable resolution improvement achieved after given time averaging (e.g. [2]). In the second part of the talk I will show how analysis of spin angular momentum of light can be associated with blood flow tracking and of glucose sensing. The glucose due to the structure of its molecules affects the spin angular momentum of the back scattered photons since it interacts differently with circular right and circular left polarization states of light. Similar analysis can assist in estimating the blood flow velocity (based on Ref. [3]).

#### **References:**

- [1]. D. Sazbon, Z. Zalevsky and E. Rivlin, "Qualitative real-time range extraction for preplanned scene partitioning using laser beam coding," Pat. Rec. Lett., 26, 1772-1781 (2005).
- [2]. A. Ilovitsh, T. Ilovitsh, E. Preter, N. Levanon and Z. Zalevsky, "Super resolution using Barker-based array projected via spatial light modulator," Opt. Lett. 40, 1802-1805 (2015).
- [3]. D. Fixler and Z. Zalevsky, "In vivo Tumor Detection Using Polarization and Wavelength Reflection Characteristics of Gold Nanorods," Nano Lett. 13, 6292-6296 (2013).

## VORTEX-ATOM INTERACTION: OAM TRANSFER TO AN ATOMIC SAMPLE AND ITS RETRIEVAL

Laurence PRUVOST\*

<sup>1</sup>*Laboratoire Aimé Cotton, CNRS, Univ-Paris-Sud, ENS-Cachan, Univ Paris-Saclay, Orsay, France*

Keywords: vortex–atom interaction, optical angular momentum memory

Vortex beams are known for the orbital angular momentum (OAM) that they carry. This quantity is quantized by an integer  $\ell$  related to their helical phase structure and can encode the information. In the context of quantum technology, the interaction between the quantum variable of a vortex and atoms is explored by many groups to understand which processes can be relevant for transfer, storage or retrieval.

In experiments realized in collaboration with Tabosa's group (university of Recife) we have performed a memory for OAMs in a cold Caesium atomic sample provided by a magneto-optical trap. Using a delayed four-wave-mixing process applied to a  $\Lambda$  atomic system we have demonstrated that the OAM can be retrieved in a beam having a direction different from the incident writing one [1]. Using the coherent population oscillation process we have shown the robustness of the storage/retrieval against magnetic field and the possibility to compute OAMs during the nonlinear process [2].

In experiments realized in Orsay, we have induced a non-degenerated four-wave-mixing process on rubidium atoms to showing the OAM transfer with a change of frequency (red to blue) and for large values of  $\ell$ .

- [1] Off-axis retrieval of orbital angular momentum of light stored in cold atoms, R. A. de Oliveira, L. Pruvost, P. S. Barbosa, W. S. Martins, S. Barreiro, D. Felinto, D. Bloch, J. W. R. Tabosa, Appl. Phys. B, 117, 1123, 2014
- [2] Storage of orbital angular momenta of light via coherent population oscillation, A. J. F. de Almeida, S. Barreiro, W. S. Martins, R. A. de Oliveira, D. Felinto, L. Pruvost, and J. W. R. Tabosa, Opt. Lett. 40, 2545, 2015

## **OCT FOR THE DIAGNOSIS AND TREATMENT MONITORING OF CERVICAL CANCER**

Natalia SHAKHOVA

*Institute of Applied Physics RAS, Uljanov St.46, Nizhny Novgorod, Russia;*

Keywords: cervical neoplasia, noninvasive diagnosis, OCT, PS OCT, organ preserving treatment, therapy monitoring.

A significant increase in the cervical cancer incidence is observed for women of the reproductive age [1]. The “gold standard” for cervical neoplasia diagnosis is histological evaluation of colposcopy guided biopsy. However, the diagnostic efficacy of the colposcopy is limited. Similar colposcopic abnormalities can be observed for a variety of cervical conditions, benign and malignant, which reduces specificity and positive predictive value [2]. Such a situation requires new approaches and development of new techniques in order to ensure adequate diagnosing in early stage and, at the same time, to avoid over-referral to colposcopy, over-treatment and to maintain sustainable costs. Management of cervical neoplasia in reproductive age includes not only minimal invasive diagnosis, but organ preserving treatment, which requires careful planning and control. Optical coherence tomography (OCT) due to spatial resolution approaching the tissue level is capable of guiding biopsies, planning and monitoring of organ preserving treatment.

The goal of this study is to demonstrate advantages of OCT-colposcopy application for guidance of cervical biopsy, application of OCT in course of surgical resection and photodynamic therapy (PDT). The OCT device (IAP RAS) operates at 1300 nm with 3 mW power and 45 nm bandwidth. In our study we used a detachable, reusable forward-looking OCT probe with an outer diameter of 2.7 mm. Standard and polarization sensitive (PS OCT) modes were used. More than 500 female patients have been examined. The study was approved by the Ethical Committee for scientific studies with human subjects.

The previous studies revealed that the most typical OCT feature of malignization is loss of specific image structure, which allowed us to formulate features of “benign” and “malignant” OCT images [3]. This study aimed at evaluating the efficiency of OCT-colposcopy for taking a decision about cervical biopsy. Decision about biopsy was taken by a standard protocol based on colposcopy data. According to colposcopic findings 83% of cases had indications for biopsy, but only in 38% of cases malignant types of images were detected by OCT. Histology studies of biopsy material confirmed the presence of benign states in the presence of benign types of OCT images.

When choosing a method of treatment of early forms of cervical neoplasia OCT data allowed to decide on further tactics: monitoring with mild dysplasia, excision or PDT of moderate and severe forms of dysplasia.

It was shown that PS OCT can improve the specificity of diagnosis when interpreting “difficult” images.

In conclusion, in cervical neoplasia OCT makes it possible to avoid random biopsies, to validate the choice of treatment method, to plan and monitor it. At the stage of follow-up OCT allows for noninvasive evaluation of healing process and for early recurrence diagnostics.

[1] G Foley, R Alston, M Geraci, L Brabin, H Kitchener and J Birch Br. J. of Cancer, 105, 177–184 (2011)

[2] Dalla Palma P et al, Am. J. Clin. Pathol., 129(1), 75-80 (2008)

[3] N.M. Shakhova, F.I. Feldchtein, and A.M. Sergeev. In: *Handbook of Optical Coherence Tomography*, B.E. Bouma and G.I. Tearney (Eds.), Basel, Marcel Dekker, Inc., New York, 649-72 (2002)

## ENHANCEMENT OF CLINICAL APPLICATIONS OF CROSS-POLARIZATION OPTICAL COHERENCE TOMOGRAPHY BY IMAGE QUANTIFICATION

Mikhail KIRILLIN,<sup>1\*</sup> Elena KISELEVA,<sup>2</sup> Ekaterina GUBARKOVA,<sup>2</sup>  
Natalia GLADKOVA<sup>2</sup>, Ekaterina SERGEEVA<sup>1</sup>, Pavel AGRBA<sup>1</sup>, Natalia SHAKHOVA<sup>1</sup>

<sup>1</sup> *Institute of Applied Physics, Russian Academy of Sciences, 46 Ulyanov Street, Nizhny Novgorod, 603950, Russia;*

<sup>2</sup> *Nizhny Novgorod State Medical Academy, 10/1 Minin and Pozharsky Sq., Nizhny Novgorod, 603950, Russia*

Keywords: cross-polarization optical coherence tomography, clinical applications, collagen state

Optical coherence tomography (OCT) is a model noninvasive imaging modality based on principles of low-coherence interferometry which is currently actively introduced into clinical practice. Cross polarization OCT (CP OCT) is an advanced OCT modality benefiting from probing tissue with either linearly or circularly polarized light. As a result a coupled image is produced in two channels, parallel and orthogonal to initial polarization state (co- and cross-polarization channels). Employment of this modality provides additional diagnostic information due to strong dependence of probing light polarization state on the condition of collagen within probing tissue. Well-organized collagen exhibits strong birefringence that induces rotation of the polarization of probing light resulting in strong signal – cross-polarization CP OCT channel. On the contrary, disorganized collagen fibers or absence of collagen induces results in weak depolarization of the probing light and weak signal in cross-polarization channel. Thus, CP OCT is sensitive to pathologies manifested by disorders in collagen net structure.

Interpretation of diagnostic OCT images may suffer from different artifacts in OCT images which doesn't have corresponding morphological features and are caused by the principles of OCT image formation. On the other hand, some differences in OCT images may not be detected by the naked eye. Quantification of OCT images may provide additional diagnostic accuracy to OCT and help clinicians to detect alterations and biotissues in course of OCT monitoring.

In this paper we report on the approaches to quantification of diagnostic CP OCT images obtained in urologic, cardiologic, and cosmetologic applications. A special score called integral depolarization factor (IDF) was developed characterizing the average ratio of the signals in cross- and co-polarization channels of the CP OCT system. The score reflects the state of the collagen within inspected tissue as presence of organized collagen results in strong signal in cross-polarization channel. In urology CP OCT was employed for bladder diagnostics. Application of IDF allowed to reveal cancer recurrence at scar (diagnostic accuracy of 97%), fibrosis (79%), and reveal and characterize neoplasia (75%). Pathologic states accompanied by excessive collagen production demonstrated IDF value larger than that for norm, and, on the contrary, states associated with collagen disorganization and destruction demonstrated lower IDF values. In cardiology IDF allowed to differentiate between stable and vulnerable atherosclerotic plaques which is an important clinical problem. The study was performed with *post mortem* samples, however, the approach has high potential in clinical applications when an intravascular CP OCT modality will be developed. In cosmetology IDF was employed for quantification of OCT monitoring of the outcome of skin anti-ageing photodynamic therapy procedure. The approach allowed to evaluate immediate and long-term (up to 1 year) response to the procedure and has high potential in personal cosmetologic PDT planning.

The study was supported by the Russian Foundation for Basic Research (project No.15-32-20250) and by the Russian Scientific Foundation (project No.14-15-00538). The authors are grateful to REVIXAN Ltd (Moscow, Russia) for support and assistance.

## POLARIZATION DIFFERENCE IMAGING OF THE UTERINE CERVIX IN COLPOSCOPY PATIENTS

Alex J. KASS,<sup>1</sup> Mickey FRIEDMAN,<sup>2</sup> Amit SAFIR,<sup>1</sup> Ronit SLYPER,<sup>1</sup> Tzvia Dvora RUBINSHTEIN,<sup>2</sup> David LEVITZ\*,<sup>1</sup>

<sup>1</sup>*MobileODT Ltd., Gershon Shatz 41, Tel Aviv, Israel;*

<sup>2</sup>*Department of Gynecology, Rambam Health Care Campus, Haaliya Hashniya St 8, Haifa,, Israel*

Keywords: polarization difference imaging, cervical cancer, acetowhitening, scattering

Cervical cancer is the leading cause of cancer death for women in low resource settings. The high mortality is caused by a lack of access to cervical care and the absence of national screening programs. Often, nurses screen women for cervical cancer visually with the naked eye, using acetic acid as a contrast agent. In patients with cervical lesions, acetic acid turns white, suggesting the presence of dysplasia or cancer. To improve the ability of nurses to visually screen for cervical cancer, low-cost portable white light imaging instrumentation has been developed. However, screening and triage based on white light imaging has had mixed results. New methods to improve the accuracy of screeners have been proposed. One method, which has been tested *in vivo* in skin tissue, but not in cervical screening patients, is polarization difference imaging (PDI). In PDI, the tissue is illuminated with linearly polarized light and imaged at both parallel and orthogonal polarizations, or vice versa.

In this paper, the results of an exploratory clinical trial testing PDI on the cervix is presented. First, a commercial colposcope was modified to enable PDI imaging, with a liquid crystal variable retarder (LCVR) functioning as the polarizer, varying the polarization of the light on the cervix between 0° and 90°. Light returning from the tissue passed through an analyzer oriented at 0°. A data acquisition program varied the LCVR voltage to capture parallel and orthogonal images at the click of a button, and calculated and saved the PDI image, together with a normal white light image, automatically.

In the trial, women referred to colposcopy following an abnormal Pap or HPV screening test were recruited to enroll. A speculum was inserted into the vagina, giving the clinician access to the cervix. A thin layer of 5% acetic acid was brushed on the cervix using a long swab, and PDI images were acquired. The clinician determined if and where to biopsy following the standard of care. Altogether, 8 patients were recruited; 2 showed signs of dysplasia. The main difference between normal and PDI images was in the acetowhitened regions, which disappeared from the PDI images (Fig. 1). This suggests that the scattering in acetowhite regions strongly depolarized the incident light, much more than the remaining tissue. Further analyses suggests PDI can distinguish glare from acetowhitening. This feature could be of great use to nurses screening for cervical cancer in low resource settings.

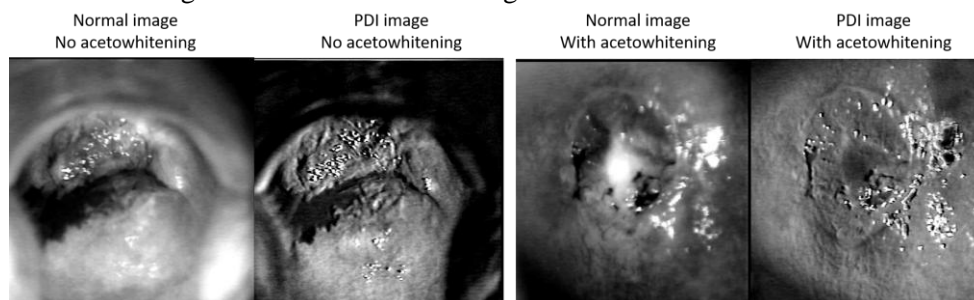


Fig. 1: Normal and PDI images, with and without acetowhitening.

## **IN VIVO MUELLER POLARIMETRIC IMAGING OF UTERINE CERVIX**

Jérémy VIZET<sup>1</sup>, Jean REHBINDER<sup>1</sup>, Stanislas DEBY<sup>1</sup>, Stéphane ROUSSEL<sup>1</sup>, André NAZAC<sup>2,3</sup>, Ranya SOUFAN<sup>4</sup>, Catherine GENESTIE<sup>4</sup>, Christine HAIE-MEDER<sup>5</sup>, Anne-Gaëlle POURCELOT<sup>2</sup>, Perrine CAPMAS<sup>2</sup>, Sylvie ZANON<sup>2</sup>, Hervé FERNANDEZ<sup>2</sup>, François MOREAU<sup>1</sup>, Angelo PIERANGELO<sup>1</sup>

<sup>1</sup>*LPICM, Ecole polytechnique, CNRS, Palaiseau 91128, France*

<sup>2</sup>*Service de Gynécologie Obstétrique, CHU de Bicêtre AP-HP, Le Kremlin-Bicêtre 94275, France*

<sup>3</sup>*Department of Obstetrics and Gynecology, University Hospital Brugmann, Université Libre de Bruxelles, Brussels, Belgium*

<sup>4</sup>*Institut Gustave Roussy, Service d'anatomie pathologique gynécologique, Villejuif 94800, France*

<sup>5</sup>*Institut Gustave Roussy, Département de Curiothérapie, Villejuif 94800, France*

Keywords: cervical cancer, polarimetry, colposcopy

Early detection through screening plays a major role in reducing the impact of cervical cancer on patients. The pre-cancerous lesions, namely, cervical intraepithelial neoplasia, can be eliminated with very limited surgery when detected before the invasive stage. The standard screening methods currently used for early detection of cervical cancer suffer from both low sensitivity and specificity. Polarimetric imaging is a promising alternative to those techniques [1]. We will present the first Mueller Polarimetric Colposcope (MPC) used for *in vivo* analysis of human uterine cervix. At probing wavelength of 550 nm our instrument enables the fast acquisition of 16 Mueller polarimetric images, thus, eliminating blur effects related to patient movement. Due to its design the MPC can also be used by a practitioner as a conventional colposcope. The MPC has been tested *in vivo* in hospital settings on a number of patients. The preliminary results of our studies are very promising and paving the way for the clinical applications of Mueller polarimetric imaging.

[1]. Rehbinder J et al "Ex vivo Mueller polarimetric imaging of the uterine cervix: a first statistical evaluation" J. Biomed. Opt. 0001;21(7):071113. doi:10.1117/1.JBO.21.7.071113.